Polymers **2015**, *7*, 1346-1378; doi:10.3390/polym7071346

OPEN ACCESS

polymers

ISSN 2073-4360

www.mdpi.com/journal/polymers

Review

From Self-Assembled Monolayers to Coatings: Advances in the Synthesis and Nanobio Applications of Polymer Brushes

Myungwoong Kim [1], Samantha K. Schmitt [2], Jonathan W. Choi [2], John D. Krutty [3] and Padma Gopalan [2,*]

[1] Department of Chemistry, Inha University, Incheon 402-751, Korea; E-Mail: mkim233@inha.ac.kr

[2] Department of Materials Science & Engineering, University of Wisconsin, Madison, WI 53706, USA; E-Mails: skschmitt@wisc.edu (S.K.S.); jchoi86@wisc.edu (J.W.C.)

[3] Department of Biomedical Engineering, University of Wisconsin, Madison, WI 53706, USA; E-Mail: krutty@wisc.edu

* Author to whom correspondence should be addressed; E-Mail: pgopalan@cae.wisc.edu; Tel.: +1-608-265-4258; Fax: +1-608-262-8353.

Academic Editor: Richard Hoogenboom

Received: 12 June 2015 / Accepted: 10 July 2015 / Published: 20 July 2015

Abstract: In this review, we describe the latest advances in synthesis, characterization, and applications of polymer brushes. Synthetic advances towards well-defined polymer brushes, which meet criteria such as: (i) Efficient and fast grafting, (ii) Applicability on a wide range of substrates; and (iii) Precise control of surface initiator concentration and hence, chain density are discussed. On the characterization end advances in methods for the determination of relevant physical parameters such as surface initiator concentration and grafting density are discussed. The impact of these advances specifically in emerging fields of nano- and bio-technology where interfacial properties such as surface energies are controlled to create nanopatterned polymer brushes and their implications in mediating with biological systems is discussed.

Keywords: polymer brush; grafting-to; solid state reaction; grafting-from; surface-initiated polymerization; reversible-deactivation radical polymerization; controlled radical polymerization; chain density; interfacial energy; nanofabrication; bio-interface; surface activity

1. Introduction

Surface anchored polymer chains are a broad class of materials where tethering of one chain end provides mechanical strength and ability to withstand a variety of post processing steps. Typically the distance between grafting points (D) is smaller than the chain end-to-end distance in the high density "brush regime". At lower grafting densities the "mushroom regime" is defined. Termed "polymer brushes", these materials have an assortment of applications and particularly, the ability to alter surface properties including bio-adhesion [1], wettability [2], modulating interfacial electronic properties [3], and surface activity [4]. Often these properties are classified under the broader term of "responsive surfaces" [5]. The responsiveness of surface constrained brushes is much larger in the moderate grafting density regime, due to greater conformational flexibility. Often the grown polymer brushes can be crosslinked to increase the mechanical robustness of the layer [6,7], allowing creation of free floating membranes with potential applications ranging from actuators to separation membranes. However, the crosslinking of these brushes to create membranes is relatively new. For example, if the stimuli-responsive nature of the polymer brushes (e.g., to pH or temperature) needs to be preserved, crosslinking the brushes is not an option as the responsiveness is compromised, instead alternate approaches based on "polymer carpets" have been developed [8,9]. The term polymer carpets was recently coined to refer to free-standing polymer brushes, grafted from a crosslinked monolayer of self-assembled initiators following photo-polymerization of suitable monomers. These are exciting developments in the field as it frees up the polymer brushes from being bound to a particular substrate making them more usable and versatile. While there are a number of review articles that have covered the various synthetic approaches for polymer brushes through polymer grafting or surface-initiated polymerization (SIP) [4,10–12], in this article we will focus on the latest advances in synthetic approaches to specifically fabricate polymer brushes independent of the substrate type and their characterization. Finally we will highlight how these advances have impacted the creation of patterned polymer brushes and their subsequent chemical modification to control tissue integration and cellular adhesion.

2. Synthetic Approaches and Challenges

To date, most fabrication strategies for polymer brushes have used one of two methods, namely "grafting-to" and "grafting-from" (Figure 1). The "grafting-to" approach involves an end-functionalized polymer chain reacting with a surface (e.g., hydroxyl-terminated polymer with an oxide surface) to anchor the polymer. Although "grafting-to" allows the polymer to be completely characterized before grafting, the method is still applicable only to a limited range of substrate types, requires the polymer chain-end to have a terminal functionality, and in general the efficiency of grafting decreases as the molecular weight increases.

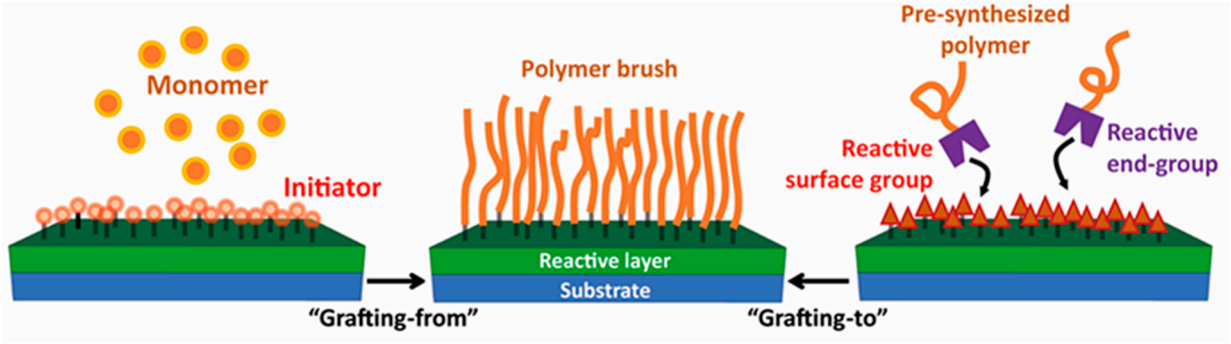

Figure 1. Scheme depicting two strategies to synthesize polymer brushes: "grafting-from" and "grafting-to" methodologies.

"Grafting-from" overcomes some of these limitations and has been used extensively with a variety of polymerization techniques such as ring-opening polymerization [13,14], ring-opening metathesis polymerization [15,16], anionic polymerization [17,18], cationic polymerization [19,20], conventional free radical polymerization [21,22], but perhaps the most widely used are the controlled radical polymerization (CRP) techniques (also called reversible-deactivation radical polymerization[23]), namely atom transfer radical polymerization (ATRP), nitroxide-mediated polymerization (NMP) and reversible addition-fragmentation chain-transfer (RAFT) polymerization [24–27]. Surface-initiated CRP has become the workhorse in the "grafting-from" literature because it is easy to polymerize a wide variety of monomers that contain an array of functional groups with a high degree of control [10]. Simply by anchoring an initiator to the appropriate substrate, polymer brushes can be grown by using polymerization conditions specific to the monomer and the anchored initiator. The vast majority of surface-anchored initiators involve the formation of a self-assembled monolayer (SAM) on an appropriate substrate [26]. While this strategy has worked well, SAMs have limited long-term stability to a variety of reagents [28–31]. Furthermore, SAMs are not substrate-independent, as they require a new initiator for every substrate type [26,32]. Moreover, when dissimilar mixed molecules are used to create a SAM, creation of a truly well-mixed layer is unlikely and difficult to access [33]. In this section, we will discuss the latest progress in synthesis of polymer brushes by "grafting-to" and "grafting-from" approaches with emphasis on efficient and fast grafting with desired grafting density, applicability to a range of substrates and complex micro- and nano-structures fabrication.

2.1. "Grafting-to" Approach

2.1.1. Solid State Grafting

A simple strategy to graft a reactive chain end onto a substrate is to thermally induce a solid state reaction that occurs at the interface between a substrate and a polymer thin film. In principle, thermal annealing of a polymer film on the substrate (typically deposited by spin-coating of a polymer solution) allows for a reactive group at the chain end to find a complementary reactive group on the surface by aiding in diffusion of polymer resulting in the formation of covalently tethered polymer brush (Figure 2a) [2,34–36]. The polymer should not have reactive side groups which can be activated during thermal annealing and cause undesired side reactions or degradation, which can occur in polymers synthesized by CRPs at elevated temperatures [37,38].

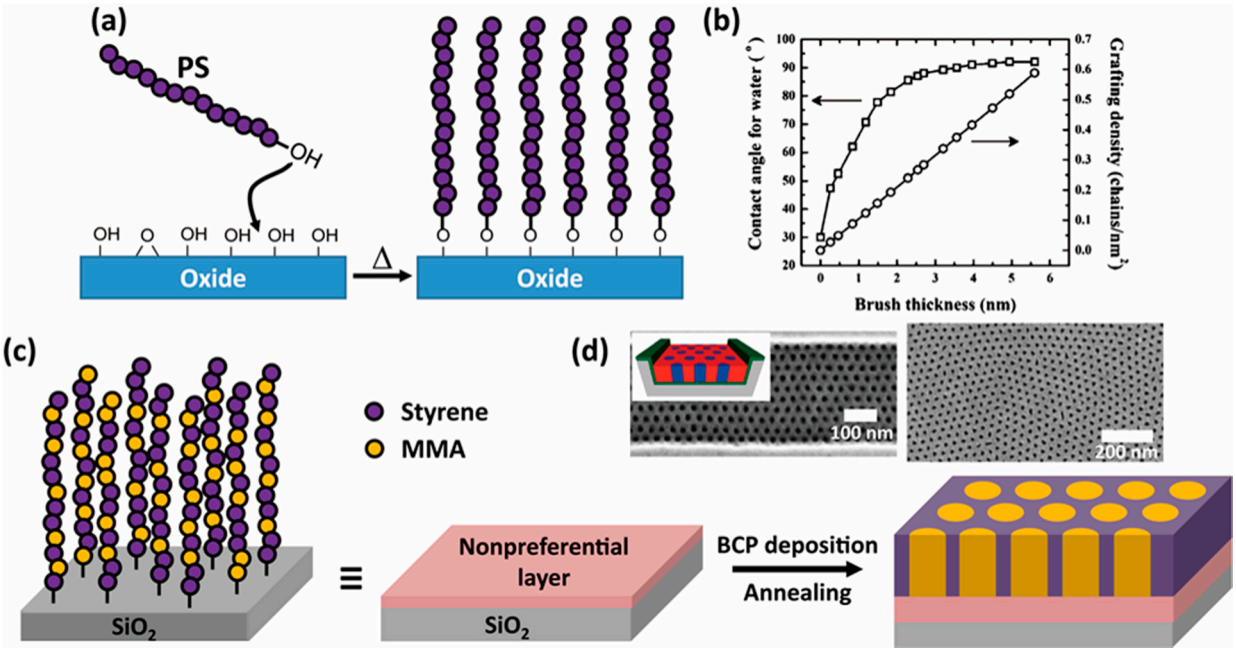

Figure 2. (**a**) Thermally induced solid state reaction for PS brush covalently bound to oxide surface; (**b**) Water contact angle and the grafting density for a series of PS brushes as a function of brush thickness showing effective control of surface energy by controlling grafting density (Reproduced with permission from Reference [39], Copyright 2011, Royal Society of Chemistry); (**c**) Creating random copolymer brush layer by thermal grafting to control wetting behavior and hence, the orientation of block copolymer; and (**d**) Top-down Scanning Electron Microscope (SEM) images of perpendicularly oriented PMMA domains (block dots in SEM images) in P(S-*b*-MMA) (poly(styrene-*block*-methyl methacrylate)) thin film on graphoepitaxial and planar substrates grafted with random copolymers. Schematic inset shows well-aligned vertically oriented PMMA cylinderss (blue) in PS matrix (red) in polymer brush (green) grafted graphoepitaxial channel (Reproduced with permission from Reference [40], Copyright 2014, Royal Society of Chemistry).

There are three factors that affect solid state grafting: (i) Annealing temperature (must be above the glass transition temperature (T_g) for chain mobility but below the melting temperature (T_m) to avoid significant dewetting); (ii) Molecular weight (longer chain slower motion and hence, slower grafting); and (iii) Annealing time. A typical example of this grafting method is a thermally activated reaction of the hydroxyl group at the chain end with the silanol group on the surface of the native oxide of the silicon wafer (Figure 2a) to form an ether bond [2,41]. Guo *et al.* showed that a chain density (0–0.61 chains/nm^2) for low M_w polystyrene (PS) brush on a silicon substrate can be achieved by varying annealing temperature (110 to 150 °C) and time (s to days) [39] (Figure 2b). This method has been effective in dialing in the right interfacial energies between a solid substrate and an overlying block copolymer (BCP) film [2,42,43], leading to perpendicularly oriented periodic microdomain arrays. These domains are useful for nanolithographic applications [44–51]. In a seminal work of Mansky *et al.*, surface-grafted a hydroxyl terminated poly(styrene-*random*-methyl methacrylate) (P(S-*r*-MMA)) brush to modify the interfacial energies between the substrate and the blocks of poly(styrene-*block*-methyl methacrylate) (P(S-*b*-MMA)) [2,40,42,52–56] (Figure 2c,d).

Faster grafting kinetics can be achieved by process optimization, for example, Liu *et al.*, demonstrated a fast grafting reaction of a hydroxyl group at the end of P(S-*r*-MMA) random copolymer on a silicon substrate by heating the samples at 250 °C for ~5 min [57]. Lupi *et al.* reported Rapid Thermal Processing (RTP) where grafting time for high chain density was very short (750 s at 230 °C up to 15 s at 310 °C) without the degradation of copolymers during processing [58] (Figure 3a). Solvent vapor assisted grafting is another approach to achieve higher grafting efficiency under mild conditions (Figure 3b). Here, a carboxyl-terminated polymer film was deposited on epoxy-functionalized surface, followed by saturation of solvent vapor and heating at a temperature far below T_g, which enhanced polymer chain mobility through plasticization [59–61]. As a result, high grafting rate and comparable grafting density to conventional solid state grafting have been achieved. This method may be useful to form brushes that degrade or are reactive at high temperatures under relatively mild conditions.

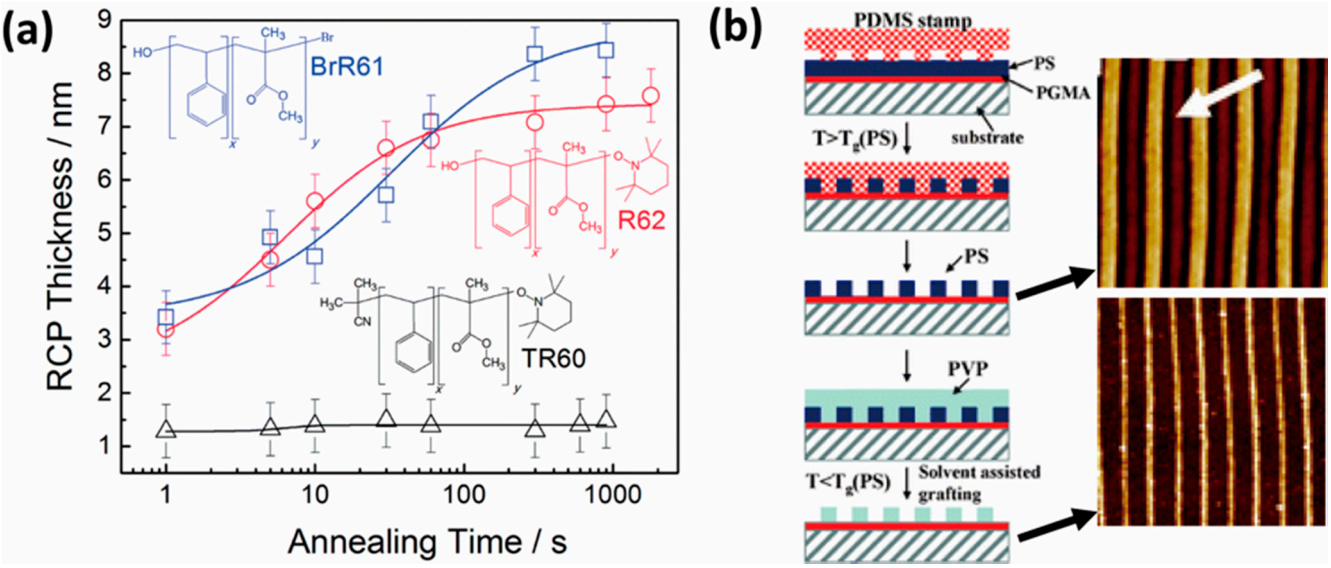

Figure 3. (**a**) Thickness of random copolymer brushes prepared via RTP at 310 °C as a function of time showing fast grafting in a short time. (Reproduced with permission from Reference [58], Copyright 2014, Royal Society of Chemistry.); and (**b**) Fabrication of patterned polymer brushes using solvent assisted grafting. White arrow indicates the grooves formed by PDMS stamp (Reproduced with permission from Reference [59], Copyright 2014, Royal Society of Chemistry).

2.1.2. Solution State Grafting

Grafting in solution is advantageous as a variety of common chemical reactions can be carried out at low temperatures, or in the presence of catalysts to promote specific grafting pathways, or on thermally unstable substrates where solid state grafting would not be possible. Examples include the use of crosslinked or multiple-point grafted poly(glycidyl methacrylate) (PGMA) thin coatings or epoxy terminated silane SAMs to attach amine- or acid-terminated polymers [62–68], a reductive alkylation reaction between amine-functionalized surface and aldehyde-terminated polymers to form an imine bond which is subsequently reduced [69,70], Au–S bond formation between thiol-terminated polymer and Au surface [71,72], thiol-disulfide exchange reaction using thiol-terminated block copolymers to prepare

for cleavable polymer brushes on silica particles [73,74], an amidation reaction of *N*-hydroxysuccinamde protected carboxylic acid terminated polymers and amine functionalized SAMs on surface [75], Diels-Alder ligation reaction between cyclopentadiene and maleimide [76], and a condensation reaction between silane-terminated polymers and silanol groups on an oxide surface [77].

More recently "Click" chemistry has been used to form polymer brushes with high grafting efficiency, minimized side reactions and to provide relatively mild reaction conditions which avoid any photochemical or thermal degradation of chemical functionalities [67,78–82]. Paoprasert *et al.* showed that Cu(I)-catalyzed Huisgen 1,3-dipolar cycloaddition of azide group with alkyne group was an efficient route to form conducting polymer brushes with controlled film thickness and chain density (Figure 4a) [78]. Yang *et al.* and Kedracki *et al.* demonstrated anchoring simple thiol-terminated PS/PMMA and thiol-terminated DNA onto complementary surfaces without any side reactions, hence preserving the DNA structure (Figure 4b) [83,84]. He *et al.* demonstrated that alkyne- or alkene-functionalized surfaces can be successfully modified with azido- or thiol-terminated poly(ionic liquid) in reasonably short time (less than an hour), showing polyelectrolyte brushes also can be formed through "grafting-to" approach with click chemistry [85]. More recently, molecular recognition between surface anchored β-cyclodextrin and azobenzene terminated polymer chains have been demonstrated to reversibly anchor and release the polymer chain in response to UV/vis light cycles [86].

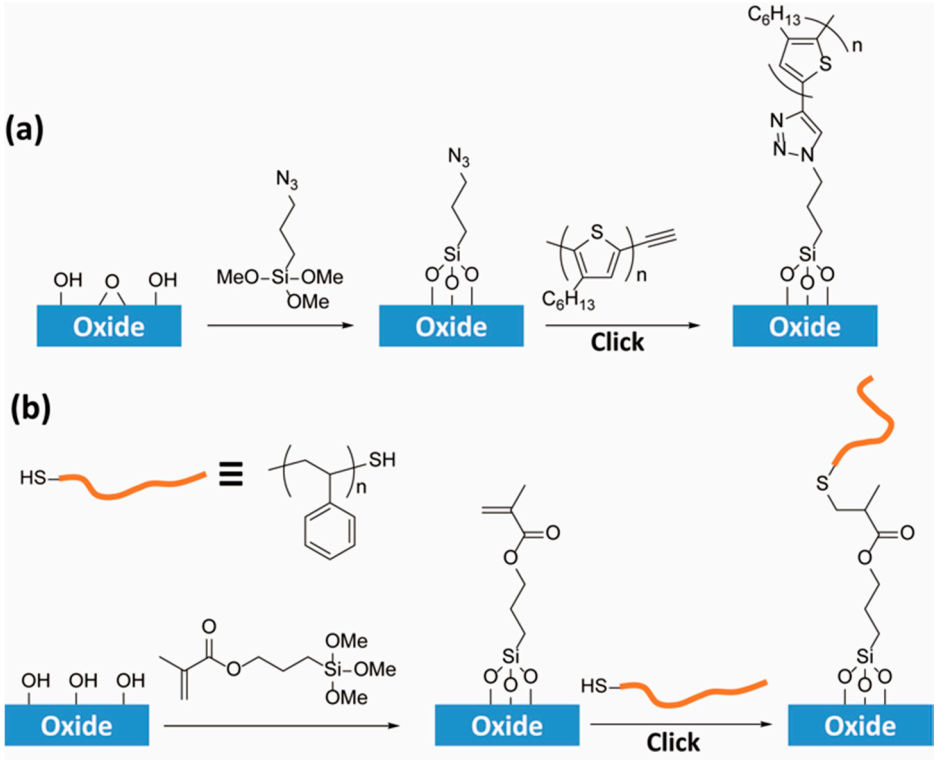

Figure 4. Examples of solution based "grafting-to" through click chemistry. (**a**) Anchoring ethynyl-terminated P3HT onto azide functionalized surface (Redrawn from Reference [78], Copyright 2010, Royal Society of Chemistry); and (**b**) Use of thiol-ene click chemistry (Redrawn from Reference [83], Copyright 2014, American Chemical Society).

2.2. "Grafting-from" Approach

2.2.1. A Conventional Approach: Creating Initiator SAMs

Self-assembled monolayers (SAMs) are widely used to define surface-anchored initiators on specific substrates, e.g., silicon (Si) and noble metals. On oxide surfaces, initiator containing silanes are immobilized, whereas on noble metal surfaces, thiol-functionalized initiators are used. However, this process cannot transverse multiple substrate types (e.g., gold to Si). Additionally, plastic substrates cannot be used as they can degrade or dissolve by soaking in initiator solutions for long periods of time (at least 12–24 h) [87,88]. Welch *et al.* demonstrated an alternate method to immobilize ATRP initiators on a conducting polymer film by vapor phase reaction of ATRP initiator with surface hydroxyl groups created by short O_2 plasma treatment [89]. Prolonged exposure to O_2 plasma typically degraded the conductivity of conducting polymer layer despite increasing the density of hydroxyl groups [88]. Another common method is direct surface-initiated photografting and photopolymerization (SIPGP) [90–92]. However, this method is only effective on organic surfaces where surface radical sites can be formed, limiting its applicability for a wide range of substrates.

2.2.2. Substrate Independent Initiator Immobilization Strategies

While the most common method for immobilizing initiators to the substrate utilizes a SAM, some alternative methods have been developed. von Werne *et al.* describe the inclusion of 10%–20% ATRP inimer (a polymerizable initiator) in a mixture of curable monomers suitable for photopolymerization [93]. This multi-component system can be used to fabricate micro- and nano-patterns through microcontact printing and nanoimprint lithography, respectively. This work was extended further by incorporation of an acid-cleavable ATRP inimer for direct comparison of the molecular weight of the surface grown brushes with the polymer grown from sacrificial initiator in solution [94]. Typically, in non-cleavable systems, the polymer brush formed is characterized only by the molecular weight of the polymer formed in solution, which relies upon kinetic assumptions discussed in Section 3.2. A different method for producing an inimer layer is to form an adhesive coating, containing chemical groups to enable initiator incorporation. For example, layers of poly(allylamine) deposited by pulsed plasma polymerization [95,96], or catechol derivatives deposited by incubation in alkaline solution to form stable polydopamine layers on various substrates were functionalized with ATRP initiators (Figure 5a) [97–104]. More simply, a thin film of thermally crosslinked PGMA was formed on a silicon wafer, after which an ATRP initiator was introduced using the remaining epoxy groups [105].

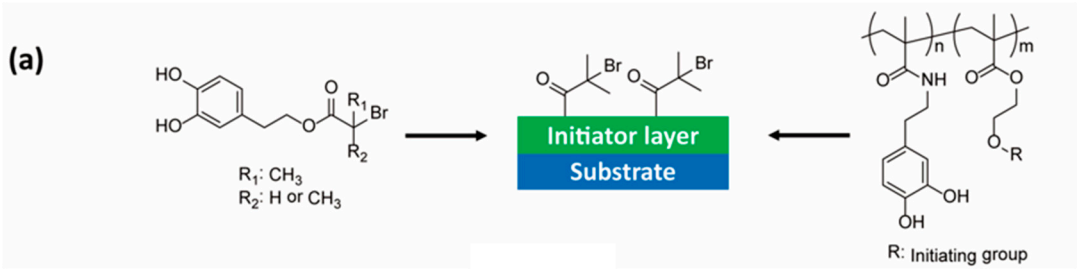

Figure 5. *Cont.*

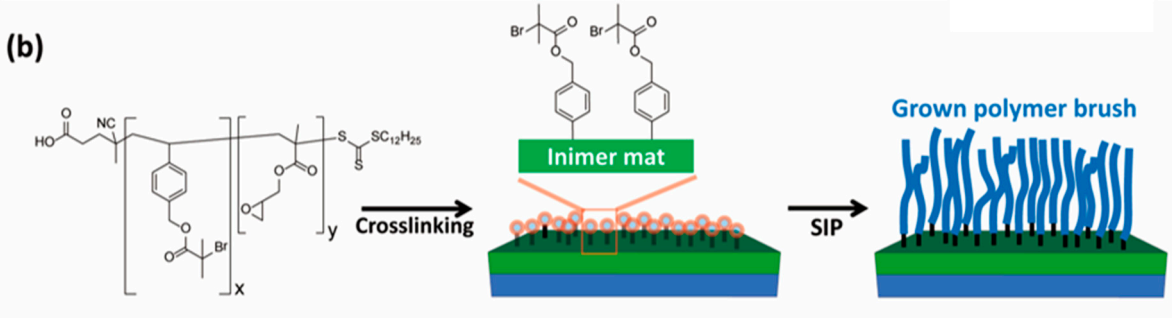

Figure 5. (**a**) Representative example of the use of catechol derivatives for initiator containing thin films [97–100,104]; and (**b**) Schematic illustration of the process for the formation of the initiator containing crosslinked thin film, followed by the brush growth (Reproduced with permission from Reference [106], Copyright 2014, American Chemical Society).

Recently, Sweat *et al.* reported a comprehensive approach that allowed growth of polymer brushes from a wide range of substrate types, with a high grafting density by using a single component system [106,107] (Figure 5b). The design involved a crosslinkable copolymer coating containing an inimer as a co-monomer. Specifically, a random copolymer composed of an inimer, *p*-(2-bromoisobutyloylmethyl)styrene (BiBMS), and a crosslinkable monomer, glycidyl methacrylate (GMA) was synthesized by RAFT polymerization. Thermal crosslinking created a coating that was stable in organic solvent and could withstand processes such as sonication and Soxhlet extraction. During the polymerization using surface-initiated ATRP (SI-ATRP) to grow PMMA brushes, a sacrificial initiator was also added to the solution. The comparison of the molecular weight of the polymer grown in solution and the layer thickness of the polymer brush, the grafting density was estimated as 0.80 ± 0.06 chains/nm^2. By comparison, this density is significantly higher than other "very dense" brushes prepared with SAMs [108]. Use of the crosslinked inimer coating prevents any problems with blend miscibility that might exist for a multi-component curable mixture, while allowing for high chain density on multiple substrate types. The growth of polymer brushes from these inimer coatings is fundamentally different from those grown from traditional SAMs, as much higher brush density and full substrate independence, is imparted by crosslinking. Furthermore, variation of the inimer coating's thickness using simple spin coating from a few nanometers to tens of microns can yield denser, more stable brushes with new and complex architectures.

2.3. Micro- and Nano-Patterned Brushes

The advances in synthetic methodologies for both "grafting-to" and "grafting-from" approaches has led to newer ways to pattern polymer brushes by the top-down, bottom-up, or a combination of both methodologies [109,110]. Nealey and coworkers have shown a top-down method to create small periodic PS brush nanopatterns on a substrate by a lithographic processes including advanced lithography and O_2 plasma etching [111–113]. A typical process involves spin-coating a photoresist on a PS brush grafted silicon substrate through "grafting-to", followed by patterning using E-beam lithography to produce line/space and dot arrays. O_2 plasma etching is used to chemically modify regions of the PS brush that are exposed therefore converting the topographic photoresist pattern into a chemical surface pattern, which can then direct the assembly of a overlying BCP film. Han *et al.* showed that the PS brushes can be replaced with P(S-*b*-MMA) and can be directly patterned without the use of O_2 plasma etching [114,115]. Surface wetting

characteristics at the nanoscale were tuned by changing the composition of the grafted BCP. The BCP brush layer was successfully patterned with a line pitch of 70 nm, which was used as a chemical pattern to direct the assembly of an overlying BCP film (Figure 6a).

Nanopatterned polymer brushes can also be fabricated through a combination of top-down and bottom-up approaches. Top-down patterning through lithography was adapted to pattern polymer brushes synthesized by bottom-up "grafting-from" approach. Rastogi *et al.* reported the direct patterning of several methacrylate-based polymer brushes that were exposed to e-beam lithography resulting in a patterned polymer brush surface [116]. Paik *et al.* further showed that e-beam patterning of P(S-*b*-MMA) brushes created by SIP led to nanochannels, as the upper layer (PS) was crosslinked (negative tone resist) and the bottom layer (PMMA) was degraded upon e-beam exposure (positive tone resist) [117] (Figure 6b).

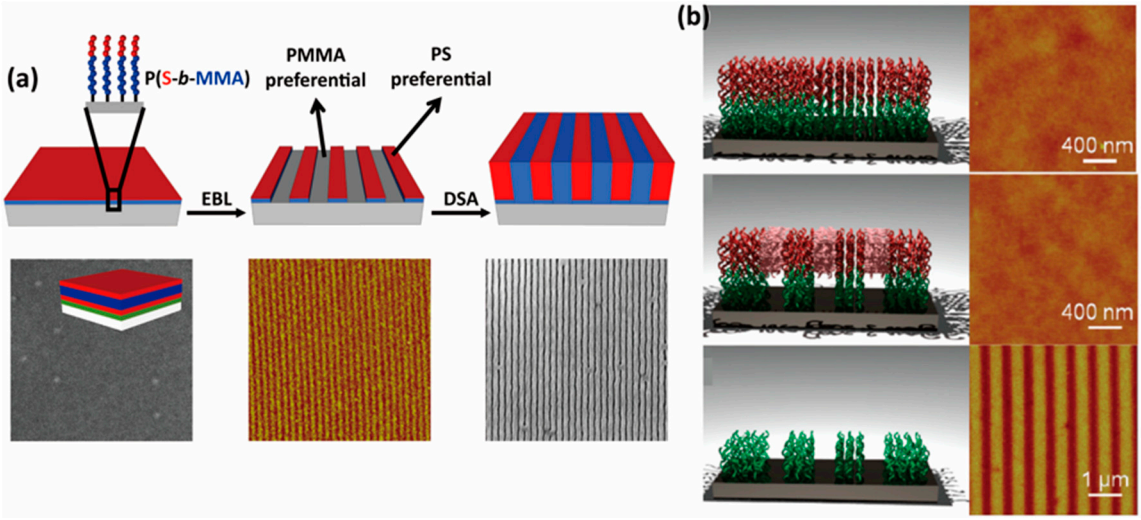

Figure 6. (**a**) Schematic illustration of the use of surface-anchored P(S-*b*-MMA) brush to fabricate chemical patterns for directed assembly of BCP. Corresponding SEM and Atomic Force Microscope (AFM) images are shown for each step. The inset schematic in the left SEM image represents parallel lamellae microdomains in the P(S-*b*-MMA) thin film (Reproduced with permission from Reference [114], Copyright 2012, American Chemical Society).; and (**b**) Nano-channels created by grafting P(S-*b*-MMA) brush (**top**) and crosslinking top PS and removing bottom PMMA in P(S-*b*-MMA) brush (**middle**). Resulting nanochannel was confirmed by etching PS layer and subsequent AFM imaging (**bottom**). The AFM images show the surface morphologies of corresponding schematic images (Reproduced with permission from Reference [117], Copyright 2010, American Chemical Society).

Although the above examples rely on top-down optical lithography to pattern brushes, recently it was shown that only the bottom-up approach (excluding all lithographic processes) can be utilized to fabricate nanopatterned polymer brushes. As shown in Figure 7, Sweat *et al.* demonstrated a dual-functional layer composed of a random copolymer consisting of an inimer (*p*-(2-bromoisobutyloylmethyl)styrene), styrene, and GMA [107]. The surface polarity was tuned through the ratio of S to inimer and GMA, to identify nonpreferential conditions to direct the assembly of an overlying cylinder forming P(S-*b*-MMA) block copolymer (BCP) film. After self-assembly, the minority PMMA domain was removed, resulting in a nanoporous template. From this pre-patterned template, in the area where the crosslinked inimer mat

was exposed, SIP was successfully carried out through by ATRP, to grow 2-hydroxylethyl methacrylate (HEMA) or poly(ethylene glycol) methyl ethyl methacrylate (PEGMEMA). By lift-off of the BCP template, a dense periodic array of brushes where each spot is about 15 nm in diameter and the density of the spots on the surface is close to 5×10^{10} cm^{-2}. The approach further shows its versatility to make more complex structures, for example, the pores formed after selective removal were filled in with gold by E-beam evaporation for Au dot arrays, followed by the lift-off of the template, resulting in Au dot arrays. In this work, the inimer containing thin film acted both as a nonpreferential layer for BCP domain orientation and as a template to grow nanopatterned brushes.

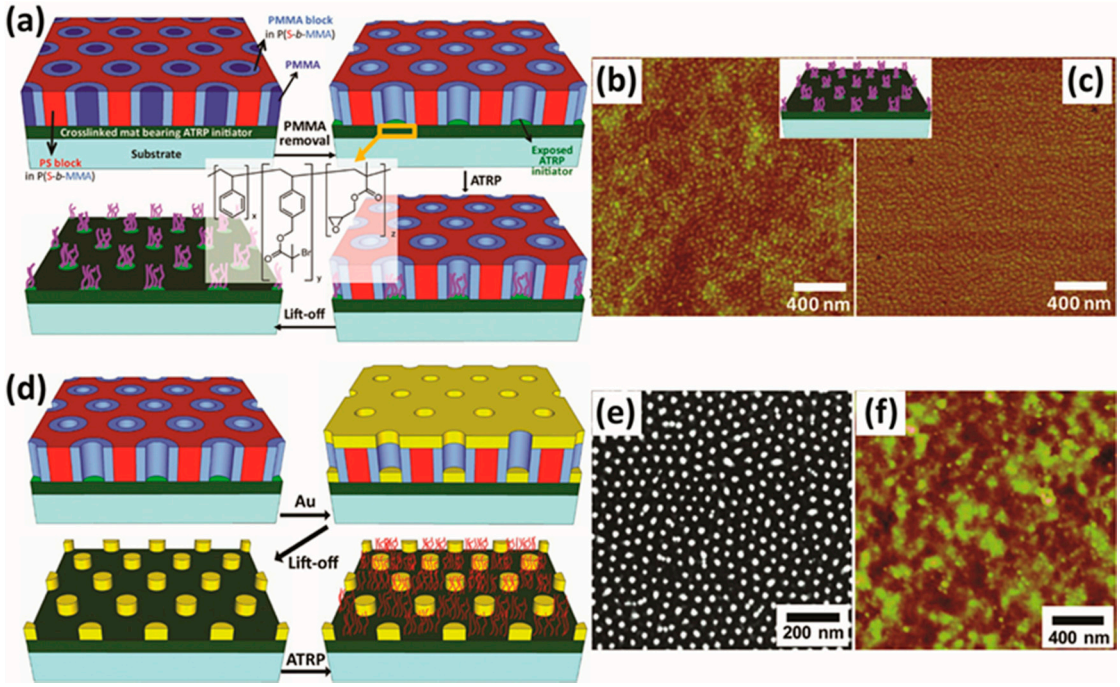

Figure 7. (**a**) The formation of a BCP template and polymer brush growth with a dual-functional initiator containing crosslinked thin film; (**b**) AFM height image of grown polymer brushes after removal of PS template; (**c**) AFM phase image of polymer brush after removal of PS template; (**d**) the fabrication of Au dot arrays with subsequent brush growth; (**e**) Top-down SEM image of Au dot arrays after template lift-off; and (**f**) AFM height image after growth of PEGMEMA (Reproduced with permission from Reference [107], Copyright 2013, American Chemical Society).

3. Challenges in Polymer Brush Characterizations

Theoretical studies have shown that grafting density or chain density (σ) is a parameter which governs the physical properties of brushes on surfaces [118]. Correlation of the physical and morphological properties of polymer brushes with theoretical predictions is possible using the chain density which can be quantitatively analyzed using experimental methods. However, there are many assumptions arising from factors that are hard to predict during grafting that often lead to less than precise and reliable estimates of chain density [119]. In this section, we discuss the challenges in chain density determination and the importance of characterizing initiator-immobilized surfaces before SIP for pre-determined properties related to the brush regime.

3.1. Chain Density

Chain density is defined as the number of polymer chains per unit area. The physical distance between grafted brushes inversely scales with chain density; hence as the distance between brushes decreases the chain density increases. When the chain density is smaller than the radius of gyration of the polymer chains, R_g, individual polymer chains start overlapping with adjacent chains, inducing strong steric hindrance, leading to increase in excluded volume and therefore, a more extended and stretched conformation of the brushes normal to the substrate [120].

Theory has shown that the chain stretching in polymer brushes correlates with the chain density through the scaling law:

$$h \propto N \cdot \sigma^{v}$$

where h is averaged length of the extended polymer chain which corresponds to the thickness of polymer brush film, N is the degree of polymerization, and v is an exponent, generally valued from 0–1 [119,121–123]. Theoretical and experimental studies have shown that the exponent v varies with the grafting density and the solvent quality [123,124]. Figure 8 shows the general scaling behavior of polymer brushes and identifies three regimes: mushroom, moderate-density brush, and high-density brush. In the mushroom regime, the average distance (D) between chains is larger than $2R_g$, resulting in v–0 [124]. However, when D is smaller than $2R_g$, the system moves into the brush regime, leading to higher v and hence a moderate-density or high-density brush regime. Experimentally, in a good solvent, when the chain density is 0.05–0.1 nm$^{-2} \leq \sigma \leq$ 0.3–0.4 nm^{-2} for PMMA (*i.e.*, moderate-density regime), v approaches 1/3. However, as the chains become more crowded (*i.e.*, high-density regime in Figure 8), e.g., $\sigma >$ 0.3–0.4 nm^{-2} for PMMA, v approaches ~0.6 in a good solvent [119]. Scaling behavior is quite different in a poor solvent and in a theta solvent: in moderate-density regime, v was found to be ~0.8 in a poor solvent and ~0.5 in theta solvent, respectively. These two values are higher than the v for moderate-chain density regime in a good solvent [119,120,125].

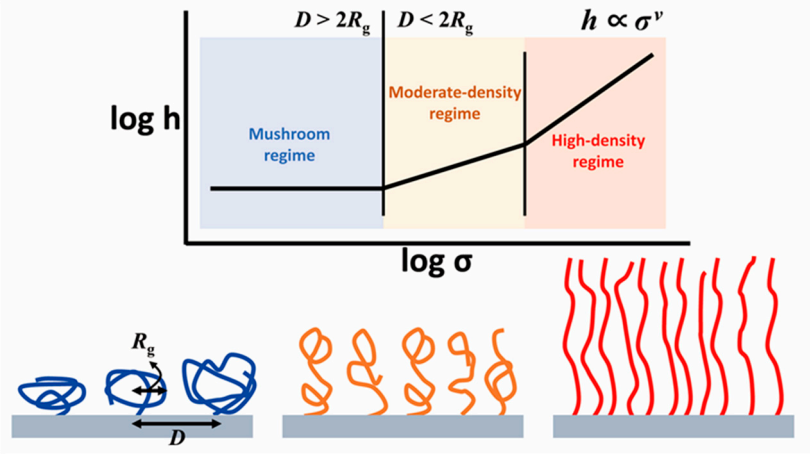

Figure 8. Schematic depicting scaling law for brush thickness and grafting density. Three different polymer brush regimes are defined (D: the distance between grafting sites). v (slope for log h *vs.* log σ plot) is dependent of solvent quality, for example, in moderate-density regime, v approaches 1/3 in a good solvent, but v approaches ~0.8 in a poor solvent and ~0.5 in a theta solvent [119].

In fact the chain density is unique for each polymer type or chemical structure. For example, a repeat unit with a bulkier pendent group, e.g., PEGMEMA, will have a lower maximum chain density (theoretical $\sigma_{max} \sim 0.17$ nm^{-2} on a planar surface) than methyl methacrylate (theoretical $\sigma_{max} \sim 1.5$ nm^{-2} on a planar surface, moderate-density regime: $\sigma > 0.3$ nm^{-2}) and therefore, the brush regime is observed at lower chain densities [106,107]. On the contrary, some rigid rod type polymers exhibit much higher chain density, for example, poly(*p*-phenylene) brushes are reported to have a chain density of 0.2–7 nm^{-2} [77].

Empirically, chain density is determined by the mass balance equation given by:

$$\sigma = (h \cdot \rho \cdot N_a)/M_n$$

where h is thickness of dry film, ρ is the bulk density of polymer, N_a is Avogadro number and M_n is the number average molecular weight of polymer. The distance between grafting sites, D, is typically correlated with σ, using the equation below:

$$D = (4/\pi \cdot \times \sigma)^{1/2}$$

The dry thickness of fabricated polymer brush films is typically measured using ellipsometry [53,114,115]. Determining σ of brushes prepared by "grafting-to" approach is straightforward, as full physical characterizations (including molecular weight determination) of a bulk sample of end-functionalized polymer can be done before actual grafting. However, in the "grafting-from", finding σ is much more challenging as polymer brushes synthesized by SIP are covalently bound to the surfaces, which complicates direct determination of the molecular weight [126,127].

3.2. Determination of Molecular Weights of Polymer Brushes

For polymer brushes synthesized by SIP, a conventional way to determine the chain density is to correlate the molecular weight of sacrificial polymer which is simultaneously polymerized from small amount of unbound free initiator in the same solution to the resulting brush layer thickness [108]. This correlation is established using a convenient assumption, namely, propagation kinetics on a two-dimensional (2D) surface is the same as the propagation kinetics in solution. The validity of this assumption has not yet been proven [128–131]. For example, Sweat *et al.* and Koylu *et al.* reported that polymers grown from sacrificial initiator in solution exhibited lower molecular weight than polymer brushes [94,106]. However, other theoretical and experimental studies reported lower molecular weights for grafted polymer brushes [128–130]. The polymerization conditions are equally critical to obtaining reasonable molecular weights and hence, a reasonable correlation to chain density [106,132].

To avoid this complication, the molecular weight information of surface grown chains can be obtained by degrafting and analysis of the chains by matrix-assisted laser desorption/ionization time of flight (MALDI-TOF) or size exclusion chromatography (SEC). This can be accomplished by direct cleavage of the chains at the grafting site (Figure 9), and requires an uniquely designed initiator with functional groups cleavable by external stimuli such as UV light [127,133], and chemical reagents which can cleave disulfides or hydrolyze ester links [94,134]. Alternatively, even though the initiator might not have cleavable groups, its bonding to the surface can be cleaved using suitable reagents. For example, initiators bound to the surface through silane chemistry ($Si_{initiator}$–O–$Si_{substrate}$ bond) or thiol-Au bonds can be cleaved using suitable reagents. Hydrofluoric acid has been one of the common reagents used for this strategy [124,135,136]. Recently, it was reported that a much milder reagent, tetrabutylammonium

fluoride (TBAF), is also effective for degrafting from silicon dioxide [126,132]. The reagent penetrates into the polymeric layers to cleave $Si_{initiator}$–O–$Si_{substrate}$ bonds, leading to degrafting of brush chains. Polymer brushes bound by thiol-Au bond can be cleaved by oxidation in iodine (I_2) solution as well [137]. These studies emphasize that molecular weight information of polymer brushes can be obtained and importantly, a reliable evaluation of chain density is feasible, even without complicated synthetic designs of cleavable initiators.

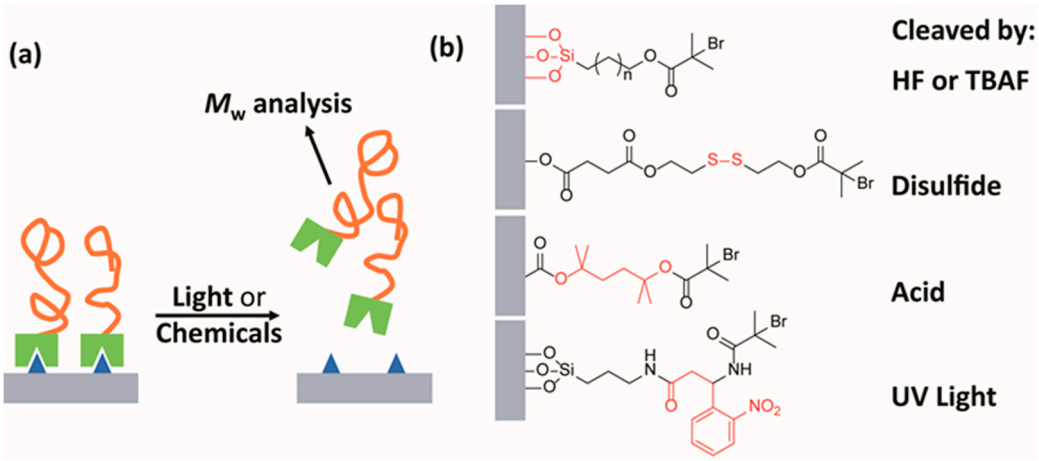

Figure 9. (**a**) Schematic depicting the cleavage of polymer brushes from the surface to obtain its molecular weight information (blue and green: cleavable functionality at the end of polymer brushes (orange)); and (**b**) Representative examples of cleavable functional groups (red-colored) by external stimuli [94,126,127,134,135].

3.3. Quantifying Surface Functional Groups: Initiator Density

As mentioned in previous sections, in order to design polymer brushes with pre-determined properties, it is crucial to understand how to quantify and control the chain density [137]. A high initiator density is required for the growth of polymer brushes with high chain density. On the contrary, lowering of the initiator density is required for the mushroom regime. One way to quantify the initiator density is by measuring the weight loss resulting from thermal decomposition [129]. Pasetto *et al.* heated up initiator-coated mesoporous silica particles to 800 °C using thermogravimetric analysis. Therefore, the surface concentration of initiator (molecule/nm^2) can be calculated by the equation:

$$\sigma_{\mathrm{I}} = \frac{\dfrac{w\%_{\mathrm{ini+silica}}}{100 - w\%_{\mathrm{ini+silica}}} - \dfrac{w\%_{\mathrm{silica}}}{100 - w\%_{\mathrm{silica}}}}{M_{ini} + S_{\mathrm{sp}}} \times N_{\mathrm{A}}$$

where *w%* is the weight loss after heating, N_A is the Avogadro's number, M_{ini} is the molar mass of the initiator and S_{sp} is the specific area measured by gas adsorption. This straightforward method is particularly useful for initiator-coated particle samples. For reliable estimates this requires a large amount of samples, hence is difficult to implement on truly 2D surfaces such as silicon wafer.

Ellipsometry and contact angle measurements have been used for the general characterization of 2D surfaces with immobilized initiators. X-ray Photoelectron Spectroscopy (XPS) can also be used for surface characterization as it probes a depth of ~10 nm. Most often XPS is used to confirm brush growth, to study surface chemical composition of the brush and to determine surface densities of bound

molecules on the brush [138–142]. XPS has also been used for initiator-coated surfaces, however most of these studies have been limited to qualitative confirmation of the presence of initiator groups [143–146].

Recently, a detailed XPS characterization of ATRP initiator containing surface was reported for the absolute initiator density estimation (*i.e.*, the number of initiators per unit volume, in this case, the number of bromine atoms per unit volume) [106]. Conventionally, XPS has been used to determine the absolute surface concentration of a particular element by integrating the intensity ratio of the element in the SAMs to that of an element in the underlying substrate, where atomic density is known [78,147]. For an ATRP initiator containing surface, contributions from the emitted electrons in three different layers to the net signal has been analyzed: Electrons emitted from elements (C, O and Br) from initiator containing organic layer, electrons emitted from silicon atoms from the native oxide layer and electrons emitted from silicon atoms in the silicon substrate (Figure 10). Taking the three layers into account in the equation of the intensity of the XPS signals, the absolute initiator density was derived from the equation:

$$N_{Br,organic} = \frac{\frac{A_{Br}}{S_{Br}}}{\frac{A_{si}}{S_{Si}}} \cdot \frac{N_{Si,SiO_2} \cdot e^{\frac{-L}{\lambda_{Si,organic} \cdot cos\theta}} \cdot \int_0^{Tox} e^{\frac{-Z}{\lambda_{Si,SiO_2} \cdot \cos\theta}}}{\int_0^{L} e^{\frac{-z}{\lambda_{Br,organic} \cdot \cos\theta}} dz}$$

where $N_{Br,organic}$ is the number density of bromine (Br/nm^2), $N_{Si,SiO2}$ is the number density of silicon atom in native oxide, A_{Br} and A_{Si} are the integrated intensity of bromine peak and silicon peak in XPS spectra, respectively, S_{Br} and S_{Si} are the relative sensitivity factors of bromine and silicon, respectively. $\lambda_{Br,organic}$, $\lambda_{Si,organic}$ and $\lambda_{Si,SiO2}$, are the inelastic mean free paths of electrons from bromine in the organic thin film layer, electrons from silicon in the organic thin film layer and electrons from silicon in native oxide layer [148,149]. T_{ox}, L, and θ are thickness of native oxide, thickness of organic layer and take-off angle of XPS measurement, respectively.

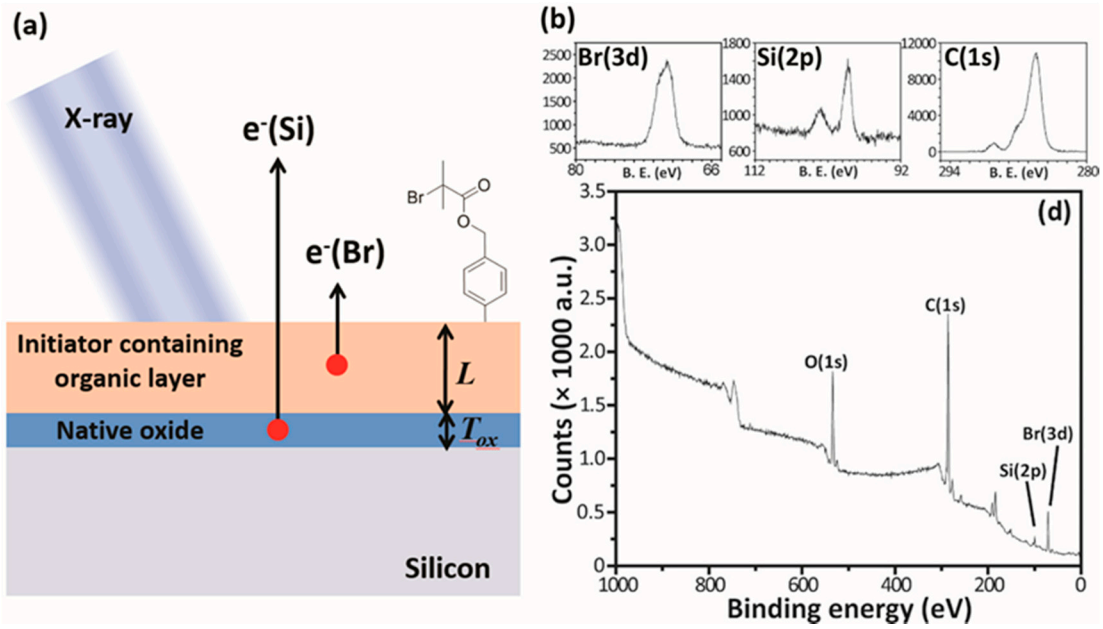

Figure 10. (**a**) XPS analysis of initiator containing organic layer on native oxide/silicon substrate; and (**b**) XPS spectra. (Reproduced with permission from Reference [106]. Copyright 2014, American Chemical Society).

Using this model the calculated initiator densities from initiator-containing organic layers were in good agreement with theoretical amounts in a unit volume. Further SI-ATRP from these surfaces showed the correlation between the high initiator density and chain density under careful optimization of the polymerization kinetics.

4. Key Applications: Imparting Functionalities in Polymer Brushes for Biomedical Applications

For biomedical engineering applications (e.g., antifouling medical devices, implant materials, biosensors and stem cell expansion), it is desirable to functionalize a surface so that it can mediate and actively dictate properties such as protein adsorption (low fouling/high fouling) and cell adhesion. Stability of polymer brushes in relatively harsh biological conditions makes them a good candidate for low fouling applications [150–152]. Polymer brushes can be modified relatively easily with peptides, proteins, or small molecules using well-defined chemistries [153] (Figure 11). This section will focus on the recent advances using polymer brushes in antifouling, biosensor, implant, and defined cell culture applications and more specifically their use as low fouling materials for selective binding of proteins, cells, antigens and tissues. For a more in depth review on biomedical applications of polymer brushes, there have been several excellent published reviews [154–156].

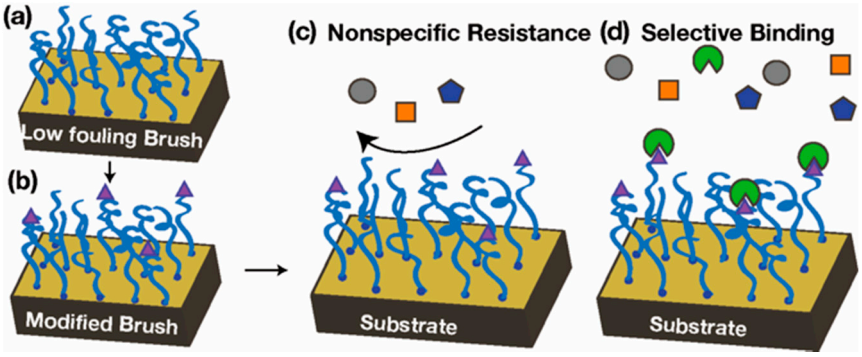

Figure 11. Schematic depiction of (**a**) low fouling polymer brush (blue lines) that is (**b**) modified with a functional molecule (purple triangles); (**c**) The functional molecules on the polymer brush do not interfere with nonspecific protein adsorption from the protein solution (circles and squares) above the brushes but allow for (**d**) selective binding of a target molecule from the solution.

4.1. Low Fouling Brushes for Controlling Material Interactions

Protein resistant surfaces are necessary for medical devices (*i.e.*, coronary stents, heart valves, catheters, and biosensors) that often come in contact with complex biological fluid such as blood, plasma, and tissue culture medium due to uncharacterized protein adsorption. This adsorption layer can lead to complications such as leukocyte adhesion or blood coagulation, which may impair the function of the device and limit its therapeutic effects [157]. Its noteworthy that as little as 10 ng/cm^2 of fibronectin can induce substantial platelet adhesion [158]. Polymer brush type, density and length are variables that can be manipulated to produce a stable, low fouling surface.

In general, polymer types that resist protein adsorption are either hydrophilic or zwitterionic, mainly due to a tightly held hydration sphere [159]. Low fouling hydrophilic materials include polyethylene

glycol, polyamides, and polysaccharides. Low fouling zwitterionic materials are classified as either polybetaines, containing a positive and negative charge on the same monomer unit, or polyampholytes, which contain a mixture of negatively and positively charged monomers. Typically quartz crystal microbalance (QCM) [160,161] or surface plasmon resonance (SPR) [162–165] using single and multicomponent solution is used for the detection of adsorbed proteins. In pursuit to minimize protein adsorption, Surman and coworkers [166] recently compared polymer brushes of poly[oligo(ethylene glycol)methyl ether methacrylate], poly(2-hydroxyethyl methacrylate) (PHEMA)), poly[*N*-(2-hydroxypropyl) methacrylamide] (PHPMA) and poly(carboxybetaine acrylamide) and their resistance to fouling when exposed to blood plasma, showing PHPMA had the best hemocompatibility with good stability, preserved for two years [167]. In an attempt to pacify some conflicting results in the literature, a more recent report compared exposure to single donor plasma *versus* plasma from several donors pooled together [168]. The SPR results between the pooled and single donor blood plasma varied up to several orders of magnitude with single donor batches while pooling resulted in more consistent data. This explains why in the literature the reported amount of protein adsorption may vary even with similar material types.

Many low fouling brush systems are grown from a SAM of ATRP initiators on gold, which leads to moderate to high brush densities. The use of gold is impractical in medical devices due to material costs and the fact that the Au-S bond is considered semi-covalent, and therefore maybe more susceptible to degradation than others [169]. However, the use of a different underlying substrate would change the brush density and therefore, the low fouling properties. (Figure 12) In fact, a study using poly(*N*,*N*-dimethylacrylamide) (PDMA) brushes found that relative fouling greatly decreased when chain density was above 0.27 chains/nm^2 and brushes were in the high density regime [170]. All brushes tested were in the brush regime with the distance D being smaller than $2R_g$, or $D/R_g < 2$.

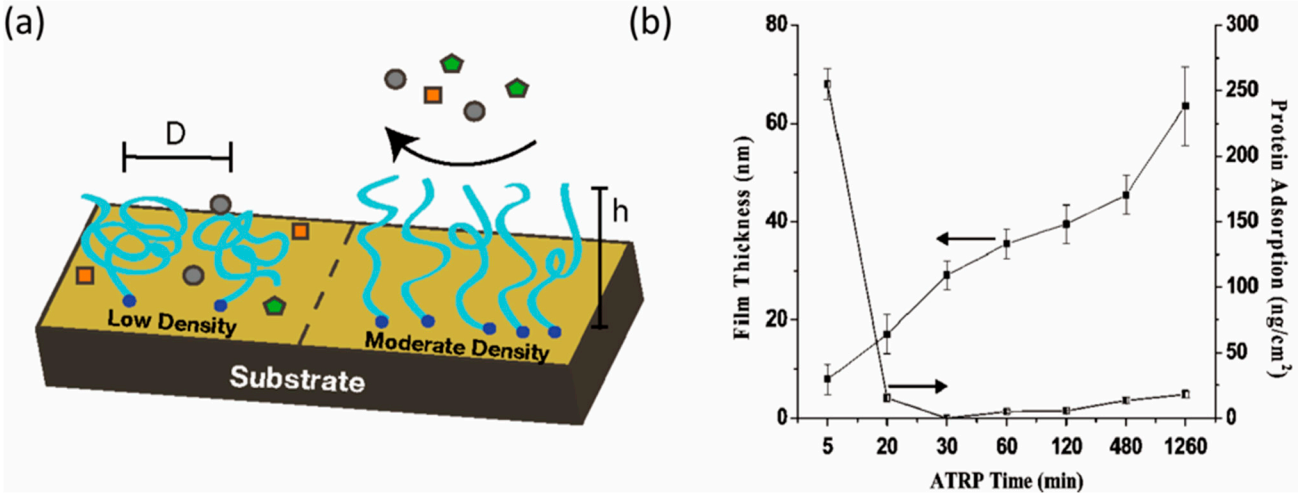

Figure 12. (**a**) Representation showing low-density polymer brushes (mushroom regime) that allow some protein adsorption and on the right moderate density brushes that prevent most proteins (squares and circles) from nonspecifically adhering. Polymer brushes are shown in blue, D is the distance between grafting points and h the height of the polymer brush. (**b**) Protein adsorption as a function of both polymerization time and film thickness of P(HMPA) surfaces measured by SPR (Reproduced with permission from Reference [171]. Copyright 2010, American Chemical Society).

Studies with PHPMA and PHEMA brushes have shown that the length of the brush can change the amount of protein adsorption when exposed to blood serum. Protein resistance continued to climb as brush length increased until 20 nm in thickness, followed by a plateau, and then it continued to increase above 40 nm [171,172]. To summarize, to create a low fouling surface, the polymer type, the polymer density and height are all important factors to create a low fouling polymer brush.

4.2. Modification and Detection of Biological Components

In some cases, it is desirable to modify a low fouling polymer brush to create a selectively binding surface. Depending on the brush type and desired application, modification using a multitude of chemistries such as "click" or carbodiimide to attach peptides, proteins, antibodies, enzymes, or nucleic acids can be done. Techniques like XPS, infrared spectroscopy (IR), quartz crystal microbalance (QCM), or SPR may be used to detect and quantify the extent of modification. Note that functionalization may occur just at the top of the polymer brush or be distributed throughout the layer. A recent depth profiling experiment using XPS looked at the profile of the modifying molecules throughout the thickness of the brush and found larger molecules only bound at the top surface of the GMA brush [173].

Cullen *et al.* used a poly(2-vinyl-4,4-dimethyl azlactone) (PVDMA) brush, which was covalently bonded to the enzyme RNase A to create a type of biosensor (Figure 13) [174]. The bound RNase A retained up to 95% of the activity of the same concentration of free enzyme. The brush platform's use was extended to other enzymes like glucose oxidase (GOx) and glycoamylase. The stability of brushes allows reusability of the sensor, whose lifetime was dependent on the stability of the enzyme on the surface.

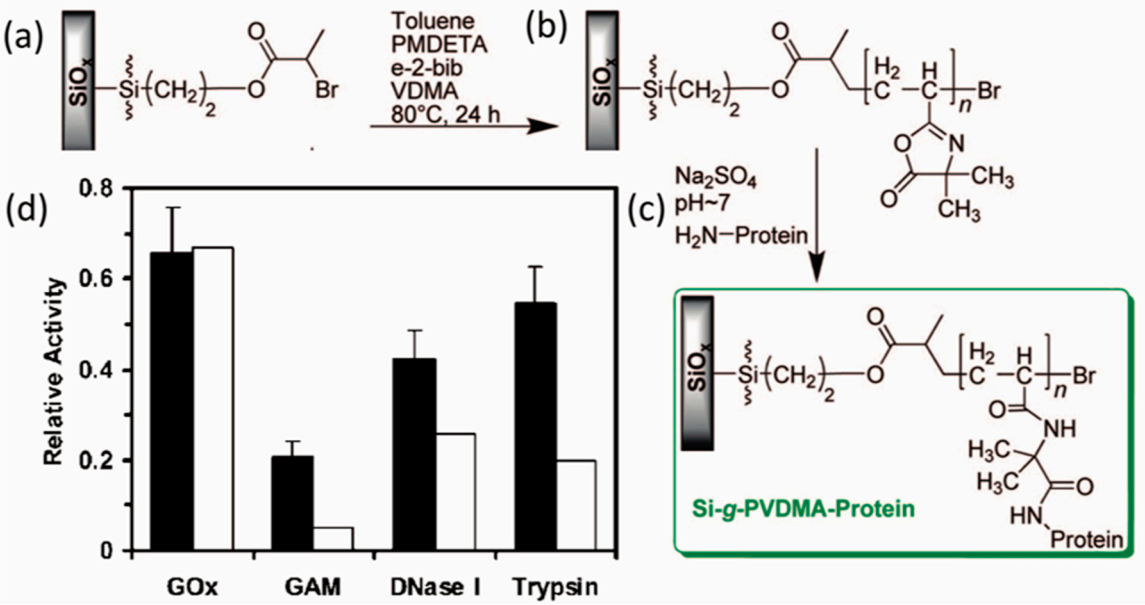

Figure 13. (**a**) Silicon surface was modified with an initiator and (**b**) PVDM brushes were grown; (**c**) The brushes were modified with multiple enzyme types by ring-opening with a primary amine on the enzyme; (**d**) The respective activities of the immobilized and free enzymes, glucose oxidase (GOx), glucoamylase (GAM), deoxyribonuclease I (DNase I) and trypsin (black bars). White bars represent comparison to other immobilization methods. (Reproduced with permission from Reference [174]. Copyright 2008, American Chemical Society).

Welch *et al.* [89] used a P(GMA-*r*-HEMA) brush tethered to the surface of poly(3,4-ethylenedioxythiophene) doped with poly(styrene sulfonate) (PEDOT:PSS) for the covalent sequestration of GOx, which was used in cooperation with a catalytic electrode to detect glucose concentrations. HEMA groups impart resistance against protein adsorption, hence increasing the selectivity and sensitivity. This system enabled highly sensitive glucose detection with long-term stability in biological fluids. HEMA provides a low fouling background, which minimizes conformational changes in the bound enzyme or protein, which can cause less effective detection of a solution target. These conformational changes can be due to nonspecific protein adsorption. In addition, disparities in polymer brush type and brush structure are also important to preserve the structure and activity of immobilized proteins [175]. Specifically, brushes with block architecture when immobilized with proteins retained the most activity and showed the least conformational changes compared to cationic, hydrophobic, and zwitterionic homopolymer brushes of the same type.

Detection methods for biosensors include, micro-ring resonators [176], voltammetry [177–179], electrochemical detection [89,92,180], interferometric detection of scattering (iSCAT) [181], as well as secondary label methods such as ELISA [182] and fluorescence [174]. Methods such as fluorescence and ELISA can have a high degree of specificity and are amenable to microarray applications allowing detection of multiple components at once (Figure 14) [183,184]. Newer techniques, like iSCAT, can achieve label-free sensing of analytes on antibody-functionalized poly(ethylene glycol) brush, to detect the presence of single unlabeled proteins without amplification, with a limit of detection (LOD) as low as 6 pM. These results far outperform other label-free sensing methods such as SPR and LPSR, which have LODs of 100 nM–1 μM. In general, label-free sensing methods are preferred to secondary label methods, offering simpler processing with fewer handling steps.

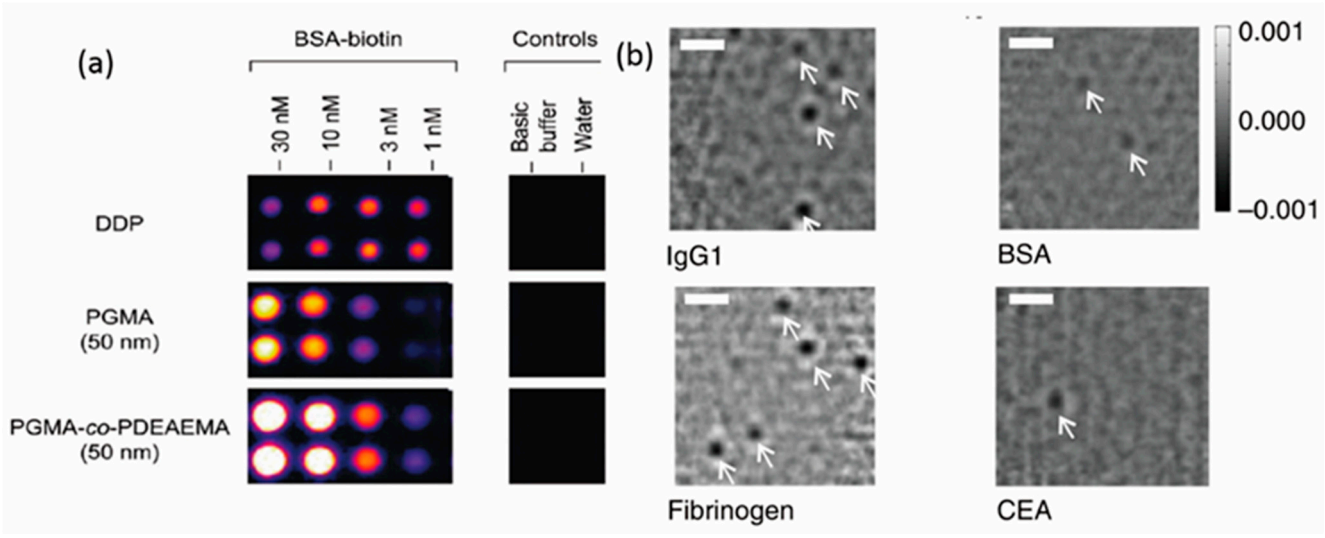

Figure 14. (**a**) Fluorescence detection on three brush types and loading intensities detected (DDP: dodecyl phosphate) (Reproduced with permission from Reference [183] Copyright 2010, American Chemical Society); and (**b**) iSCAT detection of single molecules on a polyethylene glycol brush, molecules indicated by white arrows (scale bar: 1 μm). (Reproduced with permission from Reference [181]. Copyright 2014, Nature Publications).

4.3. Controlling Cell-Material Interactions with Modified Brushes

Polymer brushes can mediate cell-material interactions either through non-specific protein adsorption or through modification of a low fouling surface to present cell adhesive peptides. On traditional polystyrene dishes, nonspecific protein adsorption is responsible for cell adhesion. A newer cell type, human pluripotent stem cells (hPSCs) are unique, as they do not adhere to traditional TCPS surfaces. hPSCs have the potential to differentiate into all of the somatic cells in the human body, and hence are promising for regenerative medicine. The current standard is to culture them on Matrigel, which is an undefined synthetic matrix that is derived from a mouse sarcoma and is subject to batch-to-batch variability as well as xenogenic contaminants. Therefore, there are efforts to find synthetic culture surfaces that can support hPSCs long-term, and are more amenable to large scale manufacturing processes. Villa-Diaz *et al.* reported the functionalization of polystyrene cell culture surfaces with polymer bushes [185]. In particular they found poly[2-(methacryloyloxy)ethyl dimethyl-(3-sulfopropyl)ammonium hydroxide] (PMEDSAH) brushes were able to support hPSCs for several passages. More recently, Qian and coworkers used PMEDSAH brushes and showed that although hPSC pluripotency was maintained on all substrates tested for five weeks, although they differ in expansion rates that depend on brush length and density [186]. Both studies rely on some protein adsorption to the polymer brushes to promote adhesion and maintenance of hPSCs. However, neither study characterized the type of adsorbed protein although this may be a key factor in understanding the cell adhesion mechanism.

To better understand how hPSCs behavior (e.g., maintenance of pluripotency) is affected by the substrate chemistry, there has been efforts to create chemically defined surfaces where a low fouling background is used in conjunction with specific peptide sequences to mimic parts of the extracellular matrix (ECM). Recently, Deng *et al.* used poly(OEGMA-*co*-HEMA) brushes with peptides to culture induced pluripotent stem cells and showed that the phenotype to be unaltered for 10 passages [187].

Orthopedic implants (e.g., prostheses, screws, plates) are used in a number of musculoskeletal conditions and diseases including bone fracture, osteoporosis, arthritis and genetic deformities. While implants may fail for a number of reasons, but they will not function at all if they do not integrate into the tissue initially. The functionalization of implant materials with polymer brushes and select extracellular matrix proteins has had an improvement on osteointegration *in vivo*. Here, instead of presenting an undefined adsorbed protein layer, researchers present a peptide on a nonfouling polymer brush background. Petrie and coworkers used 13.5 nm thick poly(oligo(ethylene glycol) methacrylate) (POEGMA) brushes grown on titanium (Ti) surfaces to immobilize a fibronectin fragment (FMIII7-10) and a shorter Arg-Gly-Asp (RGD) sequence [188]. In comparison, the fragment had better osteointegration *in vivo* than the RGD sequence, suggesting that integrin specificity is relevant, as different integrins bind to RGD and FMIII7-10. Additionally, the importance of integrin clustering was shown using monomer, dimer, trimer, and pentamers of FMIII7-10 [189]. Studies have yet to be done to investigate if polymer brush coatings can enhance osteointegration under diseased states such as osteoporosis.

Another important component of osteointegration may be growth factor signaling. Growth factors have been implicated in bone regeneration including bone morphogenetic protein (BMP, specifically BMP-2, BMP-7 and BMP-4), transforming growth factor-beta (TGF-B), vascular growth factor (VEGF), fibroblast growth factor (FGF) and platelet derived growth factor (PDGF) to name a few. Strategies employed using polymer brush surfaces include direct immobilization of growth factors or growth factor

mimics and sequestering of growth factors around the material. Ren and coworkers directly tethered fibronectin (FN) and bone morphogenic protein (BMP-2) to poly(OEGMA-*r*-HEMA) polymer brushes on Ti surfaces, shown in Figure 15.[190] While they found similar cell adhesion and proliferation, cell differentiation was increased based on alkaline phosphatase activity in comparison to pristine Ti.

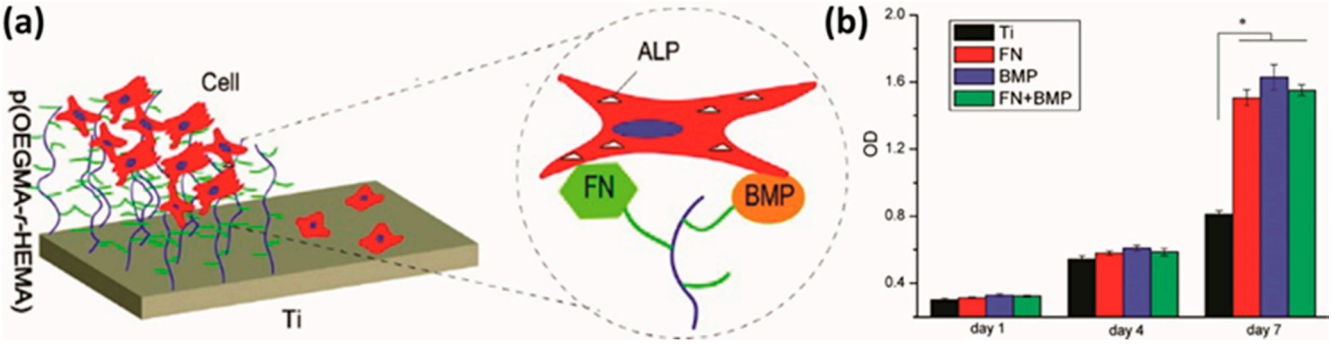

Figure 15. (**a**) Schematic depiction of P(OEGMA-HEMA) brushes on Ti functionalized directly with fibronection (FN), BMP or both FN and BMP; and (**b**) The pullout force of the modified implant material 1, 4 and 7 days after implantation. * denotes significant differences between marked groups using $p < 0.05$ with ANOVA (Reproduced with permission from Reference [190] Copyright 2011, American Chemical Society).

Although the results of direct incorporation are promising, the overall functionality of the growth factors is often reduced when it is immobilized onto a surface. Therefore, sequestering strategies where the growth factor is not modified chemically have shown the most promise. One interesting strategy, employed by Christman *et al.* [191] uses a heparin mimicking polymer brush, poly(sodium 4-styrenesulfonate-*co*-poly(ethylene glycol)) (pSS-pPEGMA), that binds the heparin domains of growth factors like bFGF and VEGF and sequesters them at the cell material interface. In a similar report, Hudalla and coworkers used a heparin binding peptide to sequester both heparin and growth factors at the cell material interface, but on a SAM surface [192]. Although these newer sequestering techniques have not been attempted *in vivo*, they could potentially improve osteointegration of implant materials, if feasible.

5. Conclusions

In this review, we have summarized recent advances in the synthesis, characterization, and applications of polymer brushes. Two different approaches to prepare for well-defined polymer brushes, "grafting-to" and "grafting-from", have been equally improved through developing new chemistries toward the goals: (i) Efficient and fast grafting; (ii) Applicability on a wide range of substrates; (iii) Precise control of surface initiator concentration and hence, chain density; and (iv) Characterizations of relevant physical parameters. These advances have impacted nano- and bio-science where control of interfacial behaviors such as altering surface energies and surface activity to regulate biologically relevant functions is the goal.

There remain significant challenges in designing more complex polymer brush structures that can orthogonally present multiple functions. The synthesis, processing and characterization of such complex brush structures, for example, mixed brushes [193–197], multiblock copolymer brushes [114,115,198], gradient polymer brushes [199,200], nanopatterned polymer brushes [107,116], polymer carpet/Janus membrane [8,201–203] and polymer nanochannels [114,117] are of great interest from a fundamental as

well as technological perspective. Comprehensive understanding of structure-property relationships in well-defined and fully characterized polymer brushes aided by new synthesis as well as predictive modeling can open up newer applications for polymer brushes.

Acknowledgments

Padma Gopalan and Samantha K. Schmitt acknowledge partial funding from the National Science Foundation (Grant No. DMR-1507409 and DMR-1306482). Jonathan W. Choi acknowledges 3M Fellowship. John D. Krutty acknowledges the Holton Fellowship from the University of Wisconsin-Madison and the Holton family. Myungwoong Kim acknowledges support from Inha University Research Grant (Grant No. INHA-51357-1).

Author Contributions

The manuscript was written through contributions of all authors. All authors have given approval to the final version of the manuscript.

Conflicts of Interest

The authors declare no conflict of interest.

References

1. Wischerhoff, E.; Uhlig, K.; Lankenau, A.; Börner, H.G.; Laschewsky, A.; Duschl, C.; Lutz, J.-F. Controlled cell adhesion on PEG-based switchable surfaces. *Angew. Chem. Int. Ed.* **2008**, *47*, 5666–5668.
2. Mansky, P.; Liu, Y.; Huang, E.; Russell, T.P.; Hawker, C. Controlling polymer-surface interactions with random copolymer brushes. *Science* **1997**, *275*, 1458–1460.
3. Zhitenev, N.B.; Sidorenko, A.; Tennant, D.M.; Cirelli, R.A. Chemical modification of the electronic conducting states in polymer nanodevices. *Nat. Nanotechnol.* **2007**, *2*, 237–242.
4. Azzaroni, O. Polymer brushes here, there, and everywhere: Recent advances in their practical applications and emerging opportunities in multiple research fields. *J. Polym. Sci. Part A* **2012**, *50*, 3225–3258.
5. Stuart, M.A.C.; Huck, W.T.S.; Genzer, J.; Müller, M.; Ober, C.; Stamm, M.; Sukhorukov, G.B.; Szleifer, I.; Tsukruk, V.V.; Urban, M.; *et al.* Emerging applications of stimuli-responsive polymer materials. *Nat. Mater.* **2010**, *9*, 101–113.
6. Welch, M.E.; Ober, C.K. Characterization of polymer brush membranes via HF etch liftoff technique. *ACS Macro Lett.* **2013**, *2*, 241–245.
7. Lilge, I.; Schönherr, H. Covalently cross-linked poly(acrylamide) brushes on gold with tunable mechanical properties via surface-initiated atom transfer radical polymerization. *Eur. Polym. J.* **2013**, *49*, 1943–1951.
8. Amin, I.; Steenackers, M.; Zhang, N.; Beyer, A.; Zhang, X.; Pirzer, T.; Hugel, T.; Jordan, R.; Gölzhäuser, A. Polymer carpets. *Small* **2010**, *6*, 1623–1630.

9. Amin, I.; Steenackers, M.; Zhang, N.; Schubel, R.; Beyer, A.; Gölzhäuser, A.; Jordan, R. Patterned polymer carpets. *Small* **2011**, *7*, 683–687.
10. Edmondson, S.; Osborne, V.L.; Huck, W.T.S. Polymer brushes via surface-initiated polymerizations. *Chem. Soc. Rev.* **2004**, *33*, 14–22.
11. Zhao, B.; Brittain, W.J. Polymer brushes: Surface-immobilized macromolecules. *Prog. Polym. Sci.* **2000**, *25*, 677–710.
12. Jennings, G.K.; Brantley, E.L. Physicochemical properties of surface-initiated polymer films in the modification and processing of materials. *Adv. Mater.* **2004**, *16*, 1983–1994.
13. Choi, I.S.; Langer, R. Surface-initiated polymerization of L-lactide: Coating of solid substrates with a biodegradable polymer. *Macromolecules* **2001**, *34*, 5361–5363.
14. Wang, Y.; Chang, Y.-C. Grafting of homo- and block co-polypeptides on solid substrates by an improved surface-initiated vapor deposition polymerization. *Langmuir* **2002**, *18*, 9859–9866.
15. Harada, Y.; Girolami, G.S.; Nuzzo, R.G. Catalytic amplification of patterning via surface-confined ring-opening metathesis polymerization on mixed primer layers formed by contact printing. *Langmuir* **2003**, *19*, 5104–5114.
16. Kong, B.; Lee, J.K.; Choi, I.S. Surface-initiated, ring-opening metathesis polymerization: Formation of diblock copolymer brushes and solvent-dependent morphological changes. *Langmuir* **2007**, *23*, 6761–6765.
17. Jordan, R.; Ulman, A.; Kang, J.F.; Rafailovich, M.H.; Sokolov, J. Surface-initiated anionic polymerization of styrene by means of self-assembled monolayers. *J. Am. Chem. Soc.* **1999**, *121*, 1016–1022.
18. Advincula, R.; Zhou, Q.; Park, M.; Wang, S.; Mays, J.; Sakellariou, G.; Pispas, S.; Hadjichristidis, N. Polymer brushes by living anionic surface initiated polymerization on flat silicon (SiO_x) and gold surfaces: Homopolymers and block copolymers. *Langmuir* **2002**, *18*, 8672–8684.
19. Jordan, R.; Ulman, A. Surface initiated living cationic polymerization of 2-oxazolines. *J. Am. Chem. Soc.* **1998**, *120*, 243–247.
20. Zhao, B.; Brittain, W.J. Synthesis of tethered polystyrene-*block*-poly(methyl methacrylate) monolayer on a silicate substrate by sequential carbocationic polymerization and atom transfer radical polymerization. *J. Am. Chem. Soc.* **1999**, *121*, 3557–3558.
21. Biesalski, M.; Rühe, J. Preparation and characterization of a polyelectrolyte monolayer covalently attached to a planar solid surface. *Macromolecules* **1999**, *32*, 2309–2316.
22. Huang, W.; Skanth, G.; Baker, G.L.; Bruening, M.L. Surface-initiated thermal radical polymerization on gold. *Langmuir* **2001**, *17*, 1731–1736.
23. Jenkins, A.D.; Jones, R.G.; Moad, G. Terminology for reversible-deactivation radical polymerization previously called "controlled" radical or "living" radical polymerization. *Pure Appl. Chem.* **2010**, *82*, 483–491.
24. Sedjo, R.A.; Mirous, B.K.; Brittain, W.J. Synthesis of polystyrene-*block*-poly(methyl methacrylate) brushes by reverse atom transfer radical polymerization. *Macromolecules* **2000**, *33*, 1492–1493.
25. Baum, M.; Brittain, W.J. Synthesis of polymer brushes on silicate substrates via reversible addition fragmentation chain transfer technique. *Macromolecules* **2002**, *35*, 610–615.

26. Barbey, R.; Lavanant, L.; Paripovic, D.; Schüwer, N.; Sugnaux, C.; Tugulu, S.; Klok, H.-A. Polymer brushes via surface-initiated controlled radical polymerization: Synthesis, characterization, properties, and applications. *Chem. Rev.* **2009**, *109*, 5437–5527.
27. Husseman, M.; Malmström, E.E.; McNamara, M.; Mate, M.; Mecerreyes, D.; Benoit, D.G.; Hedrick, J.L.; Mansky, P.; Huang, E.; Russell, T.P.; *et al.* Controlled synthesis of polymer brushes by "living" free radical polymerization techniques. *Macromolecules* **1999**, *32*, 1424–1431.
28. Flynn, N.T.; Tran, T.N.T.; Cima, M.J.; Langer, R. Long-term stability of self-assembled monolayers in biological media. *Langmuir*, **2003**, *19*, 10909–10915.
29. Strulson, M.K.; Johnson, D.M.; Maurer, J.A. Increased stability of glycol-terminated self-assembled monolayers for long-term patterned cell culture. *Langmuir* **2012**, *28*, 4318–4324.
30. Schwendel, D.; Dahint, R.; Herrwerth, S.; Schloerholz, M.; Eck, W.; Grunze, M. Temperature dependence of the protein resistance of poly- and oligo(ethylene glycol)-terminated alkanethiolate monolayers. *Langmuir* **2001**, *17*, 5717–5720.
31. Zorn, S.; Dettinger, U.; Skoda, M.W.A.; Jacobs, R.M.J.; Peisert, H.; Gerlach, A.; Chassé, T.; Schreiber, F. Stability of hexa(ethylene glycol) SAMs towards the exposure to natural light and repeated reimmersion. *Appl. Surf. Sci.* **2012**, *258*, 7882–7888.
32. Schmitt, S.K.; Murphy, W.L.; Gopalan, P. Crosslinked PEG mats for peptide immobilization and stem cell adhesion. *J. Mater. Chem. B* **2013**, *1*, 1349–1360.
33. Tong, Y.; Tyrode, E.; Osawa, M.; Yoshida, N.; Watanabe, T.; Nakajima, A.; Ye, S. Preferential adsorption of amino-terminated silane in a binary mixed self-assembled monolayer. *Langmuir* **2011**, *27*, 5420–5426.
34. Jones, R.A.L.; Lehnert, R.J.; Schonherr, H.; Vancso, J. Factors affecting the preparation of permanently end-grafted polystyrene layers. *Polymer* **1999**, *40*, 525–530.
35. Ruiz, R.; Kang, H.; Detcheverry, F.A.; Dobisz, E.; Kercher, D.S.; Albrecht, T.R.; de Pablo, J.J.; Nealey, P.F. Density multiplication and improved lithography by directed block copolymer assembly. *Science* **2008**, *321*, 936–939.
36. Bojko, A.; Andreatta, G.; Montagne, F.; Renaud, P.; Pugin, R. Fabrication of thermo-responsive nano-valve by grafting-to in melt of poly(*N*-isopropylacrylamide) onto nanoporous silicon nitride membranes. *J. Membr. Sci.* **2014**, *468*, 118–125.
37. Widin, J.M.; Kim, M.; Schmitt, A.K.; Han, E.; Gopalan, P.; Mahanthappa, M.K. Bulk and thin film morphological behavior of broad dispersity poly(styrene-*b*-methyl methacrylate) block copolymers. *Macromolecules* **2013**, *46*, 4472–4480.
38. Gianotti, V.; Antonioli, D.; Sparnacci, K.; Laus, M.; Giammaria, T.J.; Lupi, F.F.; Seguini, G.; Perego, M. On the thermal stability of PS-*b*-PMMA block and P(S-*r*-MMA) random copolymers for nanopatterning applications. *Macromolecules* **2013**, *46*, 8224–8234.
39. Guo, R.; Kim, E.; Gong, J.; Choi, S.; Ham, S.; Ryu, D.Y. Perpendicular orientation of microdomains in PS-*b*-PMMA thin films on the PS brushed substrates. *Soft Matter* **2011**, *7*, 6920–6925.
40. Kim, M.; Han, E.; Sweat, D.P.; Gopalan, P. Interplay of surface chemical composition and film thickness on graphoepitaxial assembly of asymmetric block copolymers. *Soft Matter* **2013**, *9*, 6135.
41. Park, S.-M.; Liang, X.; Harteneck, B.D.; Pick, T.E.; Hiroshiba, N.; Wu, Y.; Helms, B.A.; Olynick, D.L. Sub-10 nm nanofabrication via nanoimprint directed self-assembly of block copolymers. *ACS Nano* **2011**, *5*, 8523–8531.

42. Mansky, P.; Russell, T.P.; Hawker, C.J.; Mays, J.; Cook, D.C.; Satija, S.K. Interfacial segregation in disordered block copolymers: Effect of tunable surface potentials. *Phys. Rev. Lett.* **1997**, *79*, 237–240.
43. Huang, E.; Pruzinsky, S.; Russell, T.P. Neutrality conditions for block copolmyer systems on random copolymer brush surfaces. *Macromolecules* **1999**, *32*, 5299–5303.
44. Bai, J.; Zhong, X.; Jiang, S.; Huang, Y.; Duan, X. Graphene nanomesh. *Nat. Nanotechnol.* **2010**, *5*, 190–194.
45. Safron, N.S.; Kim, M.; Gopalan, P.; Arnold, M.S. Barrier-guided growth of micro- and nano-structured graphene. *Adv. Mater.* **2012**, *24*, 1041–1045.
46. Kim, M.; Safron, N.S.; Han, E.; Arnold, M.S.; Gopalan, P. Fabrication and characterization of large-area, semiconducting nanoperforated graphene materials. *Nano Lett.* **2010**, *10*, 1125–1131.
47. Liang, X.; Jung, Y.-S.; Wu, S.; Ismach, A.; Olynick, D.L.; Cabrini, S.; Bokor, J. Formation of bandgap and subbands in graphene nanomeshes with Sub-10 nm ribbon width fabricated via nanoimprint lithography. *Nano Lett.* **2010**, *10*, 2454–2460.
48. Kim, M.; Safron, N.S.; Han, E.; Arnold, M.S.; Gopalan, P. Electronic transport and raman scattering in size-controlled nanoperforated graphene. *ACS Nano* **2012**, *6*, 9846–9854.
49. Liang, X.; Wi, S. Transport characteristics of multichannel transistors made from densely aligned Sub-10 nm half-pitch graphene nanoribbons. *ACS Nano* **2012**, *6*, 9700–9710.
50. Choi, J.W.; Kim, M.; Safron, N.S.; Arnold, M.S.; Gopalan, P. Transfer of pre-assembled block copolymer thin film to nanopattern unconventional substrates. *ACS Appl. Mater. Interfaces* **2014**, *6*, 9442–9448.
51. Choi, J.W.; Kim, M.; Safron, N.S.; Han, E.; Arnold, M.S.; Gopalan, P. A Facile route for fabricating graphene nanoribbon array transistors using graphoepitaxy of a symmetric block copolymer. *SPIE Adv. Lithogr*. **2015**, *9428*, 94280T.
52. Ham, S.; Shin, C.; Kim, E.; Ryu, D.Y.; Jeong, U.; Russell, T.P.; Hawker, C.J. Microdomain orientation of PS-*b*-PMMA by controlled interfacial interactions. *Macromolecules* **2008**, *41*, 6431–6437.
53. Han, E.; Stuen, K.O.; La, Y.-H.; Nealey, P.F.; Gopalan, P. Effect of composition of substrate-modifying random copolymers on the orientation of symmetric and asymmetric diblock copolymer domains. *Macromolecules* **2008**, *41*, 9090–9097.
54. Chai, J.; Buriak, J.M. Using cylindrical domains of block copolymers to self-assemble and align metallic nanowires. *ACS Nano* **2008**, *2*, 489–501.
55. Han, E.; Kang, H.; Liu, C.C.; Nealey, P.F.; Gopalan, P. Graphoepitaxial assembly of symmetric block copolymers on weakly preferential substrates. *Adv. Mater.* **2010**, *22*, 4325–4329.
56. Park, S.M.; Stoykovich, M.P.; Ruiz, R.; Zhang, Y.; Black, C.T.; Nealey, P.F. Directed assembly of lamellae-forming block copolymers by using chemically and topographically patterned substrates. *Adv. Mater.* **2007**, *19*, 607–611.
57. Liu, C.-C.; Thode, C.J.; Delgadillo, P.A.R.; Craig, G.S.W.; Nealey, P.F.; Gronheid, R. Towards an all-track 300 mm process for directed self-assembly. *J. Vac. Sci. Technol. B* **2011**, *29*, 06F203.
58. Lupi, F.F.; Giammaria, T.J.; Seguini, G.; Ceresoli, M.; Perego, M.; Antonioli, D.; Gianotti, V.; Sparnacci, K.; Laus, M. Flash grafting of functional random copolymers for surface neutralization. *J. Mater. Chem. C* **2014**, *2*, 4909–4917.

59. Zdyrko, B.; Kinnan, M.K.; Chumanov, G.; Luzinov, I. Fabrication of optically active flexible polymer films with embedded chain-like arrays of silver nanoparticles. *Chem. Commun.* **2008**, 1284–1286.
60. Zdyrko, B.; Hoy, O.; Kinnan, M.K.; Chumanov, G.; Luzinov, I. Nano-patterning with polymer brushes via solvent-assisted polymer grafting. *Soft Matter* **2008**, *4*, 2213–2219.
61. Zdyrko, B.; Hoy, O.; Luzinov, I. Toward protein imprinting with polymer brushes. *Biointerphases* **2009**, *4*, FA17–FA21.
62. Drechsler, A.; Synytska, A.; Uhlmann, P.; Stamm, M.; Kremer, F. Tuning the adhesion of silica microparticles to a poly(2-vinyl pyridine) brush: An AFM force measurement study. *Langmuir* **2012**, *28*, 15555–15565.
63. Popelka, Š.; Houska, M.; Havlíková, J.; Proks, V.; Kučkaa, J.; Šturcová, A.; Bačáková, L.; Rypáčeka, F. Poly(ethylene oxide) brushes prepared by the "grafting to" method as a platform for the assessment of cell receptor-ligand binding. *Eur. Polym. J.* **2014**, *58*, 11–22.
64. Motornov, M.; Sheparovych, R.; Katz, E.; Minko, S. Chemical gating with nanostructured responsive polymer brushes: Mixed brush *versus* homopolymer brush. *ACS Nano* **2008**, *2*, 41–52.
65. Bittrich, E.; Burkert, S.; Müller, M.; Eichhorn, K.-J.; Stamm, M.; Uhlmann, P. Temperature-sensitive swelling of poly(*N*-isopropylacrylamide) brushes with low molecular weight and grafting density. *Langmuir* **2012**, *28*, 3439–3448.
66. Neubauer, N.; Winkler, R.; Tress, M.; Uhlmann, P.; Reiche, M.; Kipnusu, W.K.; Kremer, F. Glassy dynamics of poly(2-vinyl-pyridine) brushes with varying grafting density. *Soft Matter* **2015**, *11*, 3062–3066.
67. Rauch, S.; Eichhorn, K.-J.; Kuckling, D.; Stamm, M.; Uhlmann, P. Chain extension of stimuli-responsive polymer brushes: A general strategy to overcome the drawbacks of the "grafting-to" approach. *Adv. Func. Mater.* **2013**, *23*, 5675–5681.
68. Damiron, D.; Mazzolini, J.; Cousin, F.; Boisson, C.; D'Agosto, F.; Drockenmuller, E. Poly(ethylene) brushes grafted to silicon substrates. *Polym. Chem.* **2012**, *3*, 1838–1845.
69. Flavel, B.S.; Jasieniak, M.; Velleman, L.; Ciampi, S.; Luais, E.; Peterson, J.R.; Griesser, H.J.; Shapter, J.G.; Gooding, J.J. Grafting of poly(ethylene glycol) on click chemistry modified Si(100) surfaces. *Langmuir* **2013**, *29*, 8355–8362.
70. Hamilton-Brown, P.; Gengenbach, T.; Griesser, H.J.; Meagher, L. End terminal, poly(ethylene oxide) graft layers: Surface forces and protein adsorption. *Langmuir* **2009**, *25*, 9149–9156.
71. Emilsson, G.; Schoch, R.L.; Feuz, L.; Höök, F.; Lim, R.Y.H.; Dahlin, A.B. Strongly stretched protein resistant poly(ethylene glycol) brushes prepared by grafting-to. *ACS Appl. Mater. Interfaces* **2015**, *7*, 7505–7515.
72. Koutsos, V.; van der Vegte, E.W.; Hadziioannou, G. Direct view of structural regimes of end-grafted polymer monolayers: A scanning force microscopy study. *Langmuir* **1999**, *32*, 1233–1236.
73. Sun, L.; Zhao, H. Cleavage of diblock copolymer brushes in a selective solvent and fusion of vesicles self-assembled by pinned micelles. *Langmuir* **2015**, *31*, 1867–1873.
74. Zhu, S.; Li, Z.-W.; Zhao, H. Patchy micelles based on coassembly of block copolymer chains and block copolymer brushes on silica particles. *Langmuir* **2015**, *31*, 4129–4136.

75. Abbou, J.; Anne, A.; Demaille, C. Probing the structure and dynamics of end-grafted flexible polymer chain layers by combined atomic force-electrochemical microscopy. Cyclic voltammetry within nanometer-thick macromolecular poly(ethylene glycol) layers. *J. Am. Chem. Soc.* **2004**, *126*, 10095–10108.
76. Yameen, B.; Rodriguez-Emmenegger, C.; Preuss, C.M.; Pop-Georgievski, O.; Verveniotis, E.; Trouillet, V.; Rezek, B.; Barner-Kowollik, C. A facile avenue to conductive polymer brushes via cyclopentadiene–maleimide Diels–Alder ligation. *Chem. Commun.* **2013**, *49*, 8623–8625.
77. Chen, J.; Alonzo, J.; Yu, X.; Hong, K.; Messman, J.M.; Ivanov, I.; Lavrik, N.V.; Banerjee, M.; Rathore, R.; Sun, Z.; *et al.* Grafting density effects, optoelectrical properties and nano-patterning of poly(*para*-phenylene) brushes. *J. Mater. Chem. A* **2013**, *1*, 13426–13432.
78. Paoprasert, P.; Spalenka, J.W.; Peterson, D.L.; Ruther, R.E.; Hamers, R.J.; Evans, P.G.; Gopalan, P. Grafting of poly(3-hexylthiophene) brushes on oxides using click chemistry. *J. Mater. Chem.* **2010**, *20*, 2651–2658.
79. Ostaci, R.-V.; Damiron, D.; Akhrass, S.A.; Grohens, Y.; Drockenmuller, E. Poly(ethylene glycol) brushes grafted to silicon substrates by click chemistry: Influence of PEG chain length, concentration in the grafting solution and reaction time. *Polym. Chem.* **2011**, *2*, 348–354.
80. Ostaci, R.-V.; Damiron, D.; Capponi, S.; Vignaud, G.; Léger, L.; Grohens, Y.; Drockenmuller, E. Polymer brushes grafted to "passivated" silicon substrates using click chemistry. *Langmuir* **2008**, *24*, 2732–2739.
81. Hansson, S.; Trouillet, V.; Tischer, T.; Goldmann, A.S.; Carlmark, A.; Barner-Kowollik, C.; Malmström, E. Grafting efficiency of synthetic polymers onto biomaterials: A comparative study of grafting-from *versus* grafting-to. *Biomacromolecules* **2013**, *14*, 64–74.
82. Meng, D.; Sun, J.; Jiang, S.; Zeng, Y.; Li, Y.; Yan, S.; Geng, J.; Huang, Y. Grafting P3HT brushes on GO sheets: Distinctive properties of the GO/P3HT composites due to different grafting approaches. *J. Mater. Chem.* **2012**, *22*, 21583–21591.
83. Yang, K.; Huang, X.; Zhu, M.; Xie, L.; Tanaka, T.; Jiang, P. Combining RAFT polymerization and thiol–ene click reaction for core–shell structured polymer@$BaTiO_3$ nanodielectrics with high dielectric constant, low dielectric loss, and high energy storage capability. *ACS Appl. Mater. Interfaces* **2014**, *6*, 1812–1822.
84. Kedracki, D.; Chekini, M.; Maroni, P.; Schlaad, H.; Nardin, C. Synthesis and self-assembly of a DNA molecular brush. *Biomacromolecules* **2014**, *15*, 3375–3382.
85. He, H.; Averick, S.; Roth, E.; Luebke, D.; Nulwala, H.; Matyjaszewski, K. Clickable poly(ionic liquid)s for modification of glass and silicon surfaces. *Polymer* **2014**, *55*, 3330–3338.
86. Deng, J.; Liu, X.; Shi, W.; Cheng, C.; He, C.; Zhao, C. Light-triggered switching of reversible and alterable biofunctionality via β-cyclodextrin/azobenzene-based host−guest interaction. *ACS Macro Lett.* **2014**, *3*, 1130–1133.
87. Welch, M.E.; Xu, Y.; Chen, H.; Smith, N.; Tague, M.E.; Abruña, H.D.; Baird, B.; Ober, C.K. Polymer brushes as functional, patterned surfaces for nanobiotechnology. *J. Photopolym. Sci. Technol.* **2013**, *25*, 53–56.
88. He, R.-X.; Zhang, M.; Tan, F.; Leung, P.H.M.; Zhao, X.-Z.; Chan, H.L.W.; Yang, M.; Yan, F. Detection of bacteria with organic electrochemical transistors. *J. Mater. Chem.* **2012**, *22*, 22072–22076.

89. Welch, M.E.; Doublet, T.; Bernard, C.; Malliaras, G.G.; Ober, C.K. A Glucose sensor via stable immobilization of the GOx enzyme on an organic transistor using a polymer brush. *J. Polym. Sci. A* **2015**, *53*, 372–377.
90. Steenackers, M.; Gigler, A.M.; Zhang, N.; Deubel, F.; Seifert, M.; Hess, L.H.; Lim, C.H.Y.X.; Loh, K.P.; Garrido, J.A.; Jordan, R.; *et al.* Polymer brushes on graphene. *J. Am. Chem. Soc.* **2011**, *133*, 10490–10498.
91. Steenackers, M.; Küller, A.; Stoycheva, S.; Grunze, M.; Jordan, R. Structured and gradient polymer brushes from biphenylthiol self-assembled monolayers by self-initiated photografting and photopolymerization (SIPGP). *Langmuir* **2009**, *25*, 2225–2231.
92. Hess, L.H.; Lyuleeva, A.; Blaschke, B.M.; Sachsenhauser, M.; Seifert, M.; Garrido, J.A.; Deubel, F. Graphene transistors with multifunctional polymer brushes for biosensing applications. *ACS Appl. Mater. Interfaces* **2014**, *6*, 9705–9710.
93. von Werne, T.A.; Germack, D.S.; Hagberg, E.C.; Sheares, V.V.; Hawker, C.J.; Carter, K.R. A versatile method for tuning the chemistry and size of nanoscopic features by living free radical polymerization. *J. Am. Chem. Soc.* **2003**, *125*, 3831–3838.
94. Koylu, D.; Carter, K.R. Stimuli-responsive surfaces utilizing cleavable polymer brush layers. *Macromolecules* **2009**, *42*, 8655–8660.
95. Yameen, B.; Khan, H.U.; Knoll, W.; Förch, R.; Jonas, U. Surface initiated polymerization on pulsed plasma deposited polyallylamine: A polymer substrate-independent strategy to soft surfaces with polymer brushes. *Macromol. Rapid Commun.* **2011**, *32*, 1735–1740.
96. Coad, B.R.; Lua, Y.; Meagher, L. A substrate-independent method for surface grafting polymer layers by atom transfer radical polymerization: Reduction of protein adsorption. *Acta Biomater.* **2012**, *8*, 608–618.
97. Fan, X.; Lin, L.; Dalsin, J.L.; Messersmith, P.B. Biomimetic Anchor for surface-initiated polymerization from metal substrates. *J. Am. Chem. Soc.* **2005**, *127*, 15843–15847.
98. Li, C.Y.; Wang, W.C.; Xua, F.J.; Zhang, L.Q.; Yang, W.T. Preparation of pH-sensitive membranes via dopamine-initiated atom transfer radical polymerization. *J. Membr. Sci.* **2011**, *367*, 7–13.
99. Hu, H.; Yu, B.; Ye, Q.; Gu, Y.; Zhou, F. Modification of carbon nanotubes with a nanothin polydopamine layer and polydimethylamino-ethyl methacrylate brushes. *Carbon* **2010**, *48*, 2347–2353.
100. Wang, W.-C.; Wang, J.; Liao, Y.; Zhang, L.; Cao, B.; Song, G.; She, X. Surface initiated ATRP of acrylic acid on dopamine-functionalized AAO membranes. *J. Appl. Polym. Sci.* **2010**, *117*, 534–541.
101. Zhu, B.; Edmondson, S. Polydopamine-melanin initiators for surface-initiated ATRP. *Polymer* **2011**, *52*, 2141–2149.
102. Kuang, J.; Messersmith, P.B. Universal surface-initiated polymerization of antifouling zwitterionic brushes using a mussel-mimetic peptide initiator. *Langmuir* **2012**, *28*, 7258–7266.
103. Zobrist, C.; Sobocinski, J.; Lyskawa, J.; Fournier, D.; Miri, V.; Traisnel, M.; Jimenez, M.; Woisel, P. Functionalization of titanium surfaces with polymer brushes prepared from a biomimetic RAFT agent. *Macromolecules* **2011**, *44*, 5883–5892.
104. Wang, X.; Ye, Q.; Gao, T.; Liu, J.; Zhou, F. Self-assembly of catecholic macroinitiator on various substrates and surface-initiated polymerization. *Langmuir* **2012**, *28*, 2574–2581.
105. Liu, Y.; Klep, V.; Zdyrko, B.; Luzinov, I. Polymer grafting via ATRP initiated from macroinitiator synthesized on surface. *Langmuir* **2004**, *20*, 6710–6718.

106. Sweat, D.P.; Kim, M.; Yu, X.; Gopalan, P. A single-component inimer containing cross-linkable ultrathin polymer coating for dense polymer brush growth. *Langmuir* **2013**, *29*, 3805–3812.
107. Sweat, D.P.; Kim, M.; Yu, X.; Schmitt, S.K.; Han, E.; Choi, J.W.; Gopalan, P. A dual functional layer for block copolymer self-assembly and the growth of nanopatterned polymer brushes. *Langmuir* **2013**, *29*, 12858–12865.
108. Matyjaszewski, K.; Dong, H.; Jakubowski, W.; Pietrasik, J.; Kusumo, A. Grafting from surfaces for "everyone": ARGET ATRP in the presence of air. *Langmuir* **2007**, *23*, 4528–4531.
109. Chen, T.; Amin, I.; Jordan, R. Patterned Polymer Brushes. *Chem. Soc. Rev.* **2012**, *41*, 3280–3296.
110. Olivier, A.; Meyer, F.; Raquez, J.-M.; Damman, P.; Dubois, P. Surface-initiated controlled polymerization as a convenient method for designing functional polymer brushes: From self-assembled monolayers to patterned surfaces. *Prog. Polym. Sci.* **2012**, *37*, 157–181.
111. Onses, M.S.; Ramirez-Hernandez, A.; Hur, S.-M.; Sutanto, E.; Williamson, L.; Alleyne, A.G.; Nealey, P.F.; de Pablo, J.J.; Rogers, J.A. Block copolymer assembly on nanoscale patterns of polymer brushes formed by electrohydrodynamic jet printing. *ACS Nano* **2014**, *8*, 6606–6613.
112. Onses, M.S.; Song, C.; Williamson, L.; Sutanto, E.; Ferreira, P.M.; Alleyne, A.G.; Nealey, P.F.; Ahn, H.; Rogers, J.A. Hierarchical patterns of three-dimensional block-copolymer films formed by electrohydrodynamic jet printing and self-assembly. *Nat. Nanotechnol.* **2013**, *8*, 667–675.
113. Ji, S.; Liu, C.C.; Liu, G.; Nealey, P.F. Molecular transfer printing using block copolymers. *ACS Nano* **2010**, *4*, 559–609.
114. Han, E.; Kim, M.; Gopalan, P. Chemical patterns from surface grafted resists for directed assembly of block copolymers. *ACS Nano* **2012**, *6*, 1823–1829.
115. Han, E.; Leolukman, M.; Kim, M.; Gopalan, P. Resist free patterning of nonpreferential buffer layers for block copolymer lithography. *ACS Nano* **2010**, *4*, 6527–6534.
116. Rastogi, A.; Park, M.Y.; Tanaka, M.; Ober, C.K. Direct patterning of intrinsically electron beam sensitive polymer brushes. *ACS Nano* **2010**, *4*, 771–780.
117. Paik, M.Y.; Xu, Y.; Rastogi, A.; Tanaka, M.; Yi, Y.; Ober, C.K. Patterning of polymer brushes. A direct approach to complex, sub-surface structures. *Nano Lett.* **2010**, *10*, 3873–3879.
118. Binder, K.; Milchev, A. Polymer brushes on flat and curved surfaces: How computer simulations can help to test theories and to interpret experiments. *J. Polym. Sci. Part B* **2012**, *50*, 1515–1555.
119. Moh, L.C.H.; Losego, M.D.; Braun, P.V. Solvent quality effects on scaling behavior of poly(methyl methacrylate) brushes in the moderate- and high-density regimes. *Langmuir* **2011**, *27*, 3698–3702.
120. Halperin, A.; Tirrell, M.; Lodge, T.P. Tethered chains in polymer microstructures. *Adv. Polym. Sci.* **1992**, *100*, 31–71.
121. De Gennes, P.G. Conformations of polymers attached to an interface. *Macromolecules* **1980**, *13*, 1069–1075.
122. Lai, P.Y.; Halperin, A. Polymer brush at high coverage. *Macromolecules* **1991**, *24*, 4981–4982.
123. Zhulina, E.B.; Borisov, O.V.; Pryamitsyn, V.A.; Birshtein, T.M. Coil-globule type transitions in polymers. 1. Collapse of layers of grafted polymer chains. *Macromolecules* **1991**, *24*, 140–149.
124. Wu, T.; Efimenko, K.; Genzer, J. Combinatorial study of the mushroom-to-brush crossover in surface anchored polyacrylamide. *J. Am. Chem. Soc.* **2002**, *124*, 9394–9395.

125. Auroy, P.; Auvray, L. Collapse-stretching transition for polymer brushes: Preferential solvation. *Macromolecules* **1992**, *25*, 4134–4141.
126. Patil, R.R.; Turgman-Cohen, S.; Šrogl, J.; Kiserow, D.; Genzer, J. On-demand degrafting and the study of molecular weight and grafting density of poly(methyl methacrylate) brushes on flat silica substrates. *Langmuir* **2015**, *31*, 2372–2381.
127. Kang, C.; Crockett, R.M.; Spencer, N.D. Molecular-weight determination of polymer brushes generated by SI-ATRP on flat surfaces. *Macromolecules* **2014**, *47*, 269–275.
128. Gorman, C.B.; Petrie, R.J.; Genzer, J. Effect of substrate geometry on polymer molecular weight and polydispersity during surface-initiated polymerization. *Macromolecules* **2008**, *41*, 4856–4865.
129. Pasetto, P.; Blas, H.; Audouin, F.; Boissière, C.; Sanchez, C.; Save, M.; Charleux, B. Mechanistic insight into surface-initiated polymerization of methyl methacrylate and styrene via ATRP from ordered mesoporous silica particles. *Macromolecules* **2009**, *42*, 5983–5995.
130. Turgman-Cohen, S.; Genzer, J. Simultaneous bulk- and surface-initiated controlled radical polymerization from planar substrates. *J. Am. Chem. Soc.* **2011**, *133*, 17567–17569.
131. Turgman-Cohen, S.; Genzer, J. Computer simulation of concurrent bulk- and surface-initiated living polymerization. *Macromolecules* **2012**, *45*, 2128–2137.
132. Patil, R.R.; Turgman-Cohen, S.; Šrogl, J.; Kiserow, D.; Genzer, J. Direct measurement of molecular weight and grafting density by controlled and quantitative degrafting of surface-anchored poly(methyl methacrylate). *ACS Macro Lett.* **2015**, *4*, 251–254.
133. Morandi, G.; Thielemans, W. Synthesis of cellulose nanocrystals bearing photocleavable grafts by ATRP. *Polym. Chem.* **2012**, *3*, 1402–1407.
134. Hansson, S.; Antoni, P.; Bergenudd, H.; Malmström, E. Selective cleavage of polymer grafts from solid surfaces: Assessment of initiator content and polymer characteristics. *Polym. Chem.* **2011**, *2*, 556–558.
135. Von Werne, T.A.; Patten, T.E. Atom transfer radical polymerization from nanoparticles: A tool for the preparation of well-defined hybrid nanostructures and for understanding the chemistry of controlled/"living" radical polymerizations from surfaces. *J. Am. Chem. Soc.* **2001**, *123*, 7497–7505.
136. Ejaz, M.; Tsujii, Y.; Fukuda, T. Controlled grafting of a well-defined polymer on a porous glass filter by surface-initiated atom transfer radical polymerization. *Polymer* **2001**, *42*, 6811–6815.
137. Jones, D.M.; Brown, A.A.; Huck, W.T.S. Surface-initiated polymerizations in aqueous media: Effect of initiator density. *Langmuir* **2002**, *18*, 1265–1269.
138. Matrab, T.; Chehimi, M.M.; Pinson, J.; Slomkowski, S.; Basinska, T. Growth of polymer brushes by atom transfer radical polymerization on glassy carbon modified by electro-grafted initiators based on aryl diazonium salts. *Surf. Interface Anal.* **2006**, *38*, 565–568.
139. Lee, S.H.; Dreyer, D.R.; An, J.; Velamakanni, A.; Piner, R.D.; Park, S.; Zhu, Y.; Kim, S.O.; Bielawski, C.W.; Ruoff, R.S. Polymer brushes via controlled, surface-initiated atom transfer radical polymerization (ATRP) from graphene oxide. *Macromol. Rapid Commun.* **2010**, *31*, 281–288.
140. Andruzzi, L.; Hexemer, A.; Li, X.; Ober, C.K.; Kramer, E.J.; Galli, G.; Chiellini, E.; Fischer, D.A. Control of surface properties using fluorinated polymer brushes produced by surface-initiated controlled radical polymerization. *Langmuir* **2004**, *20*, 10498–10506.
141. Cedeno, D.; Krawicz, A.; Doak, P.; Yu, M.; Neaton, J.B.; Moore, G.F. Using molecular design to control the performance of hydrogen-producing polymer-brush-modified photocathodes. *J. Phys. Chem. Lett.* **2014**, *5*, 3222–3226.

142. Desseaux, S.; Klok, H.-A. Fibroblast adhesion on ECM-derived peptide modified poly(2-hydroxyethyl methacrylate) brushes: Ligand co-presentation and 3D-localization. *Biomaterials* **2015**, *44*, 24–35.
143. Ma, H.; Wells, M.; Beebe, T.P.; Chilkoti, A. Surface-initiated atom transfer radical polymerization of oligo(ethylene glycol) methyl methacrylate from a mixed self-assembled monolayer on gold. *Adv. Func. Mater.* **2006**, *16*, 640–648.
144. Tugulu, S.; Barbey, R.; Harms, M.; Fricke, M.; Volkmer, D.; Rossi, A.; Klok, H.-A. Synthesis of poly(methacrylic acid) brushes via surface-initiated atom transfer radical polymerization of sodium methacrylate and their use as substrates for the mineralization of calcium carbonate. *Macromolecules* **2007**, *40*, 168–177.
145. Xu, D.; Yu, W.H.; Kang, E.T.; Neoh, K.G. Functionalization of hydrogen-terminated silicon via surface-initiated atom-transfer radical polymerization and derivatization of the polymer brushes. *J. Colloid Interface Sci.* **2004**, *279*, 78–87.
146. Yu, K.; Wang, H.; Xue, L.; Han, Y. Stimuli-responsive polyelectrolyte block copolymer brushes synthesized from the Si wafer via atom-transfer radical polymerization. *Langmuir* **2007**, *23*, 1443–1452.
147. Franking, R.A.; Landis, E.C.; Hamers, R.J. Highly stable molecular layers on nanocrystalline anatase TiO_2 through photochemical grafting. *Langmuir* **2009**, *25*, 10676–10684.
148. Powell, C.J.; Jablonski, A. Evaluation of electron inelastic mean free paths for selected elements and compounds. *Surf. Interface Anal.* **2000**, *29*, 108–114.
149. Laibinis, P.E.; Bain, C.D.; Whitesides, G.M. Attenuation of photoelectrons in monolayers of normal-alkanethiols adsorbed on copper, silver, and gold. *J. Phys. Chem.* **1991**, *95*, 7017–7021.
150. Tugulu, S.; Klok, H.-A. Stability and nonfouling properties of poly(poly(ethylene glycol) methacrylate) brushes under cell culture conditions. *Biomacromolecules* **2008**, *9*, 906–912.
151. Kobayashi, M.; Takahara, A. Tribological properties of hydrophilic polymer brushes under wet conditions. *Chem. Rec.* **2010**, *10*, 208–216.
152. Lavanant, L.; Pullin, B.; Hubbell, J.A.; Klok, H.-A. A facile strategy for the modification of polyethylene substrates with non-fouling, bioactive poly(poly(ethylene glycol) methacrylate) brushes. *Macromol. Biosci.* **2010**, *10*, 101–108.
153. Hermanson, G.T. *Bioconjugate Techniques*; Academic Press: New York, NY, USA, 2013.
154. Krishnamoorthy, M.; Hakobyan, S.; Ramstedt, M.; Gautrot, J.E. Surface-initiated polymer brushes in the biomedical field: Applications in membrane science, biosensing, cell culture, regenerative medicine and antibacterial coatings. *Chem. Rev.* **2014**, *114*, 10976–11026.
155. Chen, S.; Li, L.; Zhao, C.; Zheng, J. Surface hydration: Principles and applications toward low-fouling/nonfouling biomaterials. *Polymer* **2010**, *51*, 5283–5293.
156. Moroni, L.; Gunnewiek, M.K.; Benetti, E.M. Polymer brush coatings regulating cell behavior: Passive interfaces turn into active. *Acta Biomater.* **2014**, *10*, 2367–2378.
157. Gorbet, M.B.; Sefton, M.V. Biomaterial-associated thrombosis: Roles of coagulation factors, complement, platelets and leukocytes. *Biomaterials* **2004**, *25*, 5681–5703.
158. Shen, M.; Wagner, M.S.; Castner, D.G.; Ratner, B.D.; Horbett, T.A. Multivariate surface analysis of plasma-deposited tetraglyme for reduction of protein adsorption and monocyte adhesion. *Langmuir* **2003**, *19*, 1692–1699.

159. Herrwerth, S.; Eck, W.; Reinhardt, S.; Grunze, M. Factors that determine the protein resistance of oligoether self-assembled monolayers—Internal hydrophilicity, terminal hydrophilicity, and lateral packing density. *J. Am. Chem. Soc.* **2003**, *125*, 9395–9366.
160. Kurosawa, S.; Aizawa, H.; Talib, Z.A.; Atthoff, B.; Hilborn, J. Synthesis of tethered-polymer brush by atom transfer radical polymerization from a plasma-polymerized-film-coated quartz crystal microbalance and its application for immunosensors. *Biosens. Bioelectron.* **2004**, *20*, 1165–1176.
161. Delcroix, M.F.; Demoustier-Champagne, S.; Dupont-Gillain, C.C. Quartz crystal microbalance study of ionic strength and pH-dependent polymer conformation and protein adsorption/desorption on PAA, PEO, and mixed PEO/PAA brushes. *Langmuir* **2014**, *30*, 268–277.
162. Yang, W.; Xue, H.; Li, W.; Zhang, J.; Jiang, S. Pursuing "zero" protein adsorption of poly(carboxybetaine) from undiluted blood serum and plasma. *Langmuir* **2009**, *25*, 11911–11916.
163. Kambhampati, D.K.; Jakob, T.A.M.; Robertson, J.W.; Cai, M.; Pemberton, J.E.; Knoll, W. Novel silicon dioxide sol–gel films for potential sensor applications: A surface plasmon resonance study. *Langmuir* **2001**, *17*, 1169–1175.
164. Wang, J.; Han, H.; Jiang, X.; Huang, L.; Chen, L.; Li, N. Quantum dot-based near-infrared electrochemiluminescent immunosensor with gold nanoparticle-graphene nanosheet hybrids and silica nanospheres double-assisted signal amplification. *Anal. Chem.* **2012**, *84*, 4893–4899.
165. Kitano, H.; Anraku, Y.; Shinohara, H. Sensing capabilities of colloidal gold monolayer modified with a phenylboronic acid-carrying polymer brush. *Biomacromolecules* **2006**, *7*, 1065–1071.
166. Surman, F.; Riedel, T.; Bruns, M.; Kostina, N.Y.; Sedláková, Z.; Rodriguez-Emmenegger, C. Polymer brushes interfacing blood as a route toward high performance blood contacting devices. *Macromol. Biosci.* **2015**, *15*, 636–646.
167. Rodriguez-Emmenegger, C.; Brynda, E.; Riedel, T.; Houska, M.; Šubr, V.; Alles, A.B.; Hasan, E.; Gautrot, J.E.; Huck, W.T.S. Polymer brushes showing non-fouling in blood plasma challenge the currently accepted design of protein resistant surfaces. *Macromol. Rapid Commun.* **2011**, *32*, 952–957.
168. Pereira, A.D.L.S.; Rodriguez-Emmenegger, C.; Surman, F.; Riedel, T.; Alles, A.B.; Brynda, E. Use of pooled blood plasmas in the assessment of fouling resistance. *RSC Adv.* **2014**, *4*, 2318–2321.
169. Ulman, A. Formation and structure of self-assembled monolayers. *Chem. Rev.* **1996**, *96*, 1533–1554.
170. Lai, B.F.L.; Creagh, A.L.; Janzen, J.; Haynes, C.A.; Brooks, D.E.; Kizhakkedathu, J.N. The induction of thrombus generation on nanostructured neutral polymer brush surfaces. *Biomaterials* **2010**, *31*, 6710–6718.
171. Zhao, C.; Li, L.; Zheng, J. Achieving highly effective nonfouling performance for surface-grafted poly(HPMA) via atom-transfer radical polymerization. *Langmuir* **2010**, *26*, 17375–17382.
172. Zhao, C.; Li, L.; Wang, Q.; Yu, Q.; Zheng, J. Effect of film thickness on the antifouling performance of poly(hydroxy-functional methacrylates) grafted surfaces. *Langmuir* **2011**, *27*, 4906–4913.
173. Barbey, R.; Laporte, V.; Alnabulsi, S.; Klok, H.-A. Postpolymerization modification of poly(glycidyl methacrylate) brushes: An XPS depth-profiling study. *Macromolecules* **2013**, *46*, 6151–6158.
174. Cullen, S.P.; Mandel, I.C.; Gopalan, P. Surface-anchored poly(2-vinyl-4,4-dimethyl azlactone) brushes as templates for enzyme immobilization. *Langmuir* **2008**, *24*, 13701–13709.
175. Takasu, K.; Kushiro, K.; Hayashi, K.; Iwasaki, Y.; Inoue, S.; Tamechika, E.; Takai, M. Polymer brush biointerfaces for highly sensitive biosensors that preserve the structure and function of immobilized proteins. *Sens. Actuator B* **2015**, *216*, 428–433.

176. De Vos, K.; Girones, J.; Popelka, S.; Schacht, E.; Baets, R.; Bienstman, P. SOI optical microring resonator with poly(ethylene glycol) polymer brush for label-free biosensor applications. *Biosens. Bioelectron.* **2009**, *24*, 2528–2533.
177. Welch, M.E.; Ritzert, N.L.; Chen, H.; Smith, N.L.; Tague, M.E.; Xu, Y.; Baird, B.A.; Abruña, H.D.; Ober, C.K. Generalized platform for antibody detection using the antibody catalyzed water oxidation pathway. *J. Am. Chem. Soc.* **2014**, *136*, 1879–1883.
178. Boujakhrout, A.; Sanchez, A.; Diez, P.; Jimenez-Falcao, S.; Martinez-Ruiz, P.; Pena-Alvarez, M.; Pingarron, J.M.; Villalonga, R. Decorating graphene oxide/nanogold with dextran-based polymer brushes for the construction of ultrasensitive electrochemical enzyme biosensors. *J. Mater. Chem. B* **2015**, *3*, 3518–3524.
179. Rafique, S.; Bin, W.; Bhatti, A.S. Electrochemical immunosensor for prostate-specific antigens using a label-free second antibody based on silica nanoparticles and polymer brush. *Bioelectrochemistry* **2015**, *101*, 75–83.
180. Crulhas, B.P.; Sempionatto, J.R.; Cabral, M.F.; Minko, S.; Pedrosa, V.A. Stimuli-responsive biointerface based on polymer brushes for glucose detection. *Electroanalysis* **2014**, *26*, 815–822.
181. Piliarik, M.; Sandoghdar, V. Direct optical sensing of single unlabelled proteins and super-resolution imaging of their binding sites. *Nat. Commun.* **2014**, *5*, 4495.
182. Costantini, F.; Nascetti, A.; Scipinotti, R.; Domenici, F.; Sennato, S.; Gazza, L.; Bordi, F.; Pogna, N.; Manetti, C.; Caputo, D.; *et al.* On-chip detection of multiple serum antibodies against epitopes of celiac disease by an array of amorphous silicon sensors. *RSC Adv.* **2014**, *4*, 2073–2080.
183. Barbey, R.; Kauffmann, E.; Ehrat, M.; Klok, H.-A. Protein microarrays based on polymer brushes prepared via surface-initiated atom transfer radical polymerization. *Biomacromolecules* **2010**, *11*, 3467–3479.
184. Aied, A.; Zheng, Y.; Pandit, A.; Wang, W. DNA Immobilization and detection on cellulose paper using a surface grown cationic polymer via ATRP. *ACS Appl. Mater. Interfaces* **2012**, *4*, 826–831.
185. Villa-Diaz, L.G.; Nandivada, H.; Ding, J.; Nogueira-de-Souza, N.C.; Krebsbach, P.H.; O'Shea, K.S.; Lahann, J.; Smith, G.D. Synthetic polymer coatings for long-term growth of human embryonic stem cells. *Nat. Biotech.* **2010**, *28*, 581–583.
186. Qian, X.; Villa-Diaz, L.G.; Kumar, R.; Lahann, J.; Krebsbach, P.H. Enhancement of the propagation of human embryonic stem cells by modifications in the gel architecture of PMEDSAH polymer coatings. *Biomaterials* **2014**, *35*, 9581–9590.
187. Deng, Y.; Zhang, X.; Zhao, X.; Li, Q.; Ye, Z.; Li, Z.; Liu, Y.; Zhou, Y.; Ma, H.; Pan, G.; *et al.* Long-term self-renewal of human pluripotent stem cells on peptide-decorated poly(OEGMA-*co*-HEMA) brushes under fully defined conditions. *Acta Biomater.* **2013**, *9*, 8840–8850.
188. Petrie, T.A.; Raynor, J.E.; Reyes, C.D.; Burns, K.L.; Collard, D.M.; García, A.J. The effect of integrin-specific bioactive coatings on tissue healing and implant osseointegration. *Biomaterials* **2008**, *29*, 2849–2857.
189. Petrie, T.A.; Raynor, J.E.; Dumbauld, D.W.; Lee, T.T.; Jagtap, S.; Templeman, K.L.; Collard, D.M.; García, A.J. Multivalent integrin-specific ligands enhance tissue healing and biomaterial integration. *Sci. Transl. Med.* **2010**, *2*, 45ra60.

190. Ren, X.; Wu, Y.; Cheng, Y.; Ma, H.; Wei, S. Fibronectin and bone morphogenetic protein-2-decorated poly(OEGMA-*r*-HEMA) brushes promote osseointegration of titanium surfaces. *Langmuir* **2011**, *27*, 12069–12073.
191. Christman, K.L.; Vázquez-Dorbatt, V.; Schopf, E.; Kolodziej, C.M.; Li, R.C.; Broyer, R.M.; Chen, Y.; Maynard, H.D. Nanoscale growth factor patterns by immobilization on a heparin-mimicking polymer. *J. Am. Chem. Soc.* **2008**, *130*, 16585–16591.
192. Hudalla, G.A.; Koepsel, J.T.; Murphy, W.L. Surfaces that sequester serum-borne heparin amplify growth factor activity. *Adv. Mater.* **2011**, *23*, 5415–5418.
193. Horton, J.M.; Tang, S.; Bao, C.; Tang, P.; Qiu, F.; Zhu, L.; Zhao, B. Truncated wedge-shaped nanostructures formed from lateral microphase separation of mixed homopolymer brushes grafted on 67 nm silica nanoparticles: Evidence of the effect of substrate curvature. *ACS Macro Lett.* **2012**, *1*, 1061–1065.
194. Price, A.D.; Hur, S.-M.; Fredrickson, G.H.; Frischknecht, A.L.; Huber, D.L. Exploring lateral microphase separation in mixed polymer brushes by experiment and self-consistent field theory simulations. *Macromolecules* **2012**, *45*, 510–524.
195. Li, W.; Bao, C.; Wright, R.A.E.; Zhao, B. Synthesis of mixed poly(ε-caprolactone)/polystyrene brushes from Y-initiator-functionalized silica particles by surface-initiated ring-opening polymerization and nitroxide-mediated radical polymerization. *RSC Adv.* **2014**, *4*, 18772–18781.
196. Hur, S.-M.; Frischknecht, A.L.; Huber, D.L.; Fredrickson, G.H. Self-assembly in a mixed polymer brush with inhomogeneous grafting density composition. *Soft Matter* **2013**, *9*, 5341–5354.
197. Calabrese, D.R.; Ditter, D.; Liedel, C.; Blumfield, A.; Zentel, R.; Ober, C.K. Design, synthesis, and use of Y-Shaped ATRP/NMP surface tethered initiator. *ACS Macro Lett.* **2015**, *4*, 606–610.
198. Kim, J.-B.; Huang, W.; Bruening, M.L.; Baker, G.L. Synthesis of triblock copolymer brushes by surface-initiated atom transfer radical polymerization. *Macromolecules* **2002**, *35*, 5410–5416.
199. Poelma, J.E.; Fors, B.P.; Meyers, G.F.; Kramer, J.W.; Hawker, C.J. Fabrication of complex three-dimensional polymer brush nanostructures through light-mediated living radical polymerization. *Angew. Chem. Int. Ed.* **2013**, *52*, 6844–6848.
200. Coad, B.R.; Bilgic, T.; Klok, H.-A. Polymer brush gradients grafted from plasma-polymerized surfaces. *Langmuir* **2014**, *30*, 8357–8365.
201. Han, D.; Xiao, P.; Gu, J.; Chen, J.; Cai, Z.; Zhang, J.; Wang, W.; Chen, T. Polymer brush functionalized janus graphene oxide/chitosan hybrid membranes. *RSC Adv.* **2014**, *4*, 22759–22762.
202. Kelby, T.S.; Wang, M.; Huck, W.T.S. Controlled folding of 2D Au-polymer brush composites into 3D microstructures. *Adv. Func. Mater.* **2011**, *21*, 652–657.
203. Kohri, M.; Shinoda, Y.; Kohma, H.; Nannichi, Y.; Yamauchi, M.; Yagai, S.; Kojima, T.; Taniguchi, T.; Kishikawa, K. Facile synthesis of free-standing polymer brush films based on a colorless polydopamine thin layer. *Macromol. Rapid Commun.* **2013**, *34*, 1220–1224.